Universidad Carlos III de Madrid

Ciemat
Centro de Investigaciones Energéticas, Medioambientales y Tecnológicas

Bachelor in Biomedical Engineering

Bachelor Thesis
2018/2019

GENERATION OF HELPER-DEPENDENT ADENOVIRAL VECTOR FOR SKIN DISORDER

Author
Rudan Xu

Tutor
Marta García Diez

Leganés, 2019

AKNOWLEDGEMENTS

My heartfelt thanks to every person who has been involved, directly or indirectly, in the development of this work.

First and foremost, I would like to express my deep and sincere gratitude to my tutor Marta García Diez for giving me the opportunity to do this study and to work with excellent professionals. Your dynamism and motivation have deeply inspired me. And this work could not have been completed without your immense patience and knowledge.

I would also like to offer my special thanks to Rodolfo Murillas Angoiti, for his invaluble help and dedication, which have been essential for this project.

I am very grateful to all members in the Epithelial Biomedicine department for their friendship and assistance, especially Blanca Duarte.

I also want to thank my friends for their encouragement and company during these four years.

Finally, I wish to express my most profound gratitude to my caring and loving family. It was a great comfort with your unconditional support and patience.

TABLE OF CONTENTS

FIGURE INDEX

ACRONYMS

bp	Base pairs
Cas9	CRISPR associated protein 9
CIEMAT	CIEMAT: Centro de Investigaciones Medioambientales, Energéticas y Tecnológicas
CRISPR	Clustered Regularly Interspaced Short Palindromic Repeats
DEB	Dystrophic Epidermolysis Bullosa
DAPI	4′,6-DiAmidino-2-PhenylIndole
DEJ	Dermal-Epidermal Junction
DMEM	Dulbecco's Modified Eagle Medium
ECM	Extracellular Matrix
EDTA	Ethylenediaminetetraacetic Acid (sodium calcium acetate)
EEO	Electroendosmosis
EtBr	Ethidium Bromide
EudraCT	European Union Drug Regulating Authorities Clinical Trial
E80	Exon 80
FACS	fluorescence-activated cell sorting
GFP	Green Fluorescence Protein
HD	Helper-dependent
HEPES	4-(2-hydroxyethyl)-1-piperazineethanesulfonic acid
HRP	Horseradish Peroxidase
iPSC	Induced Pluripotent Stem Cells
iRES	Internal Ribosome Entry Site
ITR	Inverted Terminal Repeat
kb	Kilobase (1000 base pairs of DNA or RNA)
MOI	Multiplicity of Infection
OTC	Ornithine Transcarbamylase
PCR	Polymerase Chain Reaction
PTC	Premature Terminal Codons
RDEB	Recessive Dystrophic Epidermolysis Bullosa
TAE	Tris-Acetate-EDTA
TE	Tris-EDTA
TALENs	Transcription Activator-Like Effector-Based Nucleases
ZFNs	Zinc Finger Nucleases

BACKGROUND

1. Gene therapy based on adenoviral vectors

1.1. Gene therapy overview

Gene therapy consists of introducing foreign genetic material into cells of the patient in order to treat a specific disease, which can be a genetic disorder or cancer. Genetic disease is mainly caused by abnormalities in DNA that yields the loss function of a gene, while cancer is induced by mutated oncogenes. A general workflow in gene therapy is the following: Identification of affected or missing gene, loading the vector with the therapeutic nucleic acid, delivering it into the cytoplasm (and even into the nucleus if it is necessary) and performing the therapeutic effect (Jane Flint, Principles of Virology, Fourth Edition, 2015). Aiming to treat the different types of complications, the new genetic segment can either substitute it with a new functional copy, introduce a new gene that can cure the effect of the disease or provide the missing material.

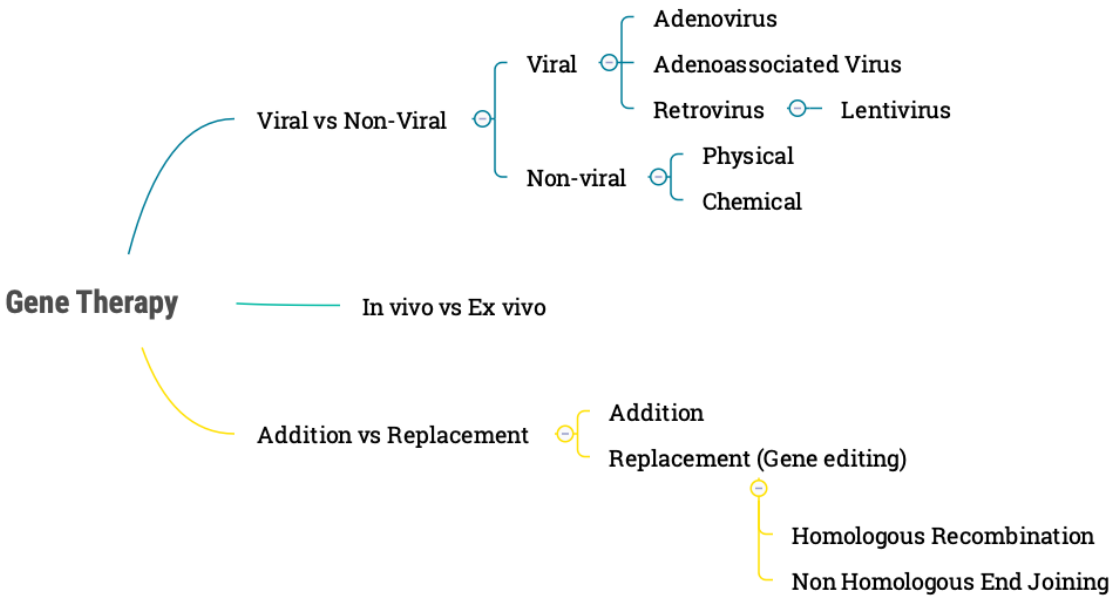

Figure 1. Gene therapy classified according to the source, administration and task.

However, the gene segment itself cannot survive inside cell on its own because it can be digested by enzymes or lysosomes present in cells, so it needs a carrier for its delivery and later therapeutic work. The role of carriers or vectors is extremely important, since it is responsible not only for carrying the gene to the right cells, but also for the gene integration and activation inside the cells. The optimal vector and delivery system varies as the target cells, the duration of expression and the length of plasmid DNA change too. According to the carriers, the delivery system can be classified as viral and non-viral.

Non-viral vectors are safer than viral ones in the term that they are not infectious and cause less immunological problems. However, the concentration of these carriers is also critical since very high amount of foreign substances can be toxic. The non-viral gene delivery uses physical methods or chemical carriers. In physical delivery system, the cell membrane is perforated or weakened for a while under physical forces and, therefore, allow the entrance of the vector-DNA complex, some examples are electroporation, hydroporation and mechanical massage. The chemical vectors can be classified according to their nature. They can be inorganic, like gold particles or calcium phosphate organic, such as lipid based, peptide based or polymer based, being the last one increasingly popular (Murali Ramamoorth, 2015). Moreover, they are also different in their loading capacity, target cells, ability to integrate the genetic material inside the nucleus and remaining period in the cell. Compared with viral methods, they have clear advantages in biosafety, but until recent years, they are not as intensively researched as viral vectors due to their main limitation: the low efficiency at delivering genes into cells.

Viruses are known by their natural ability of transducing cells by introducing their own genetic material and force the cells to synthesize viral components necessary for the package and viral proliferation. The eukaryotic viruses are therefore considered as a good candidate to deliver the genetic material into human cells. There are a wide range of viruses that can be used as gene carrier. For instance, adenovirus, adeno-associated virus and retroviruses (to which lentivirus belong) are all very well known. They considerably differ in the insertion capacity, being adenoviral the one with the largest capacity (up to 35kb), and also in transgene expression, compared in Figure 2. Even the adenoviral genome is introduced into the nucleus, it is not integrated into the host genome, so that the viral DNA will be diluted during cell division and the therapeutic effect of the transgene would be transient. In contrast, retrovirus cannot carry gene larger than 4.8kb, but its effect is stable because the gene can be integrated into the genome of the transduced cells (Lundstrom, 2018).

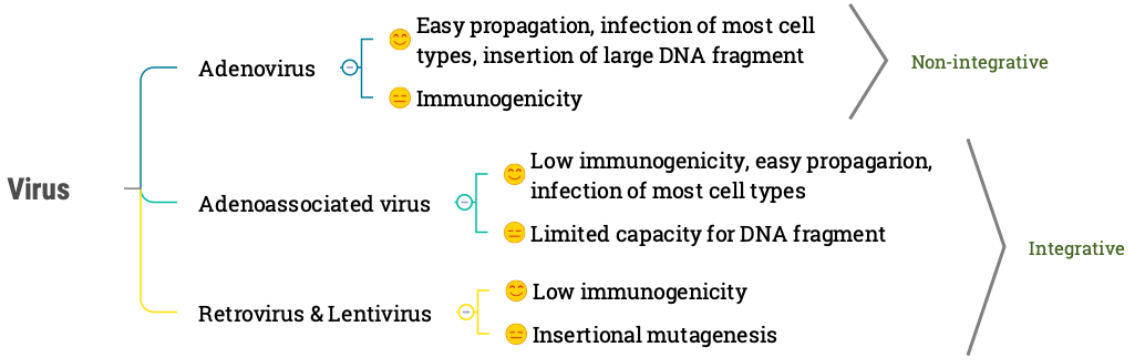

Figure 2. Advantages and limitations of different viral vectors

As during a normal viral infection, the viruses can be toxic spread through a whole tissue, they need to be cautiously manipulated before their usage, such that they cannot neither replicate nor destroy the host cells.

Besides the delivery system, the therapy can be performed *in vivo* or *ex vivo*. Taking the example of hematopoietic stem cells, *ex vivo* treatment means that the blood cells are extracted from the patient, modified by being introducing a foreign gene *in vitro*, and then transplanted back to the patient. In this way, only the extracted and purified stem cells are transfected or transduced allowing high specificity and less toxicity in the whole organism. In contrast, during *in vivo* approaches, the vectors are injected into the patient, such that the they migrate to the target cells.

Gene therapy can also be classified depending on how the gene of target cells are modified. The addition simply consists of adding a new segment to the gene, while gene editing is more complex and leading to DNA double-strand break that need to be repaired through homologous recombination (HR) and non-homologous end joining (NHEJ), as illustrated in the Figure 3. The first mechanism ensures an accurate repair because it uses the homologous template of the complementary strain. NHEJ modifies the ends of broken DNA in a random way causing possible deletions and insertions, which can be mutagenic, even though its repair is normally accurate and occurs much more commonly than HR in the nature. For organisms raised in laboratory conditions, HR is the predominant repair mechanism.

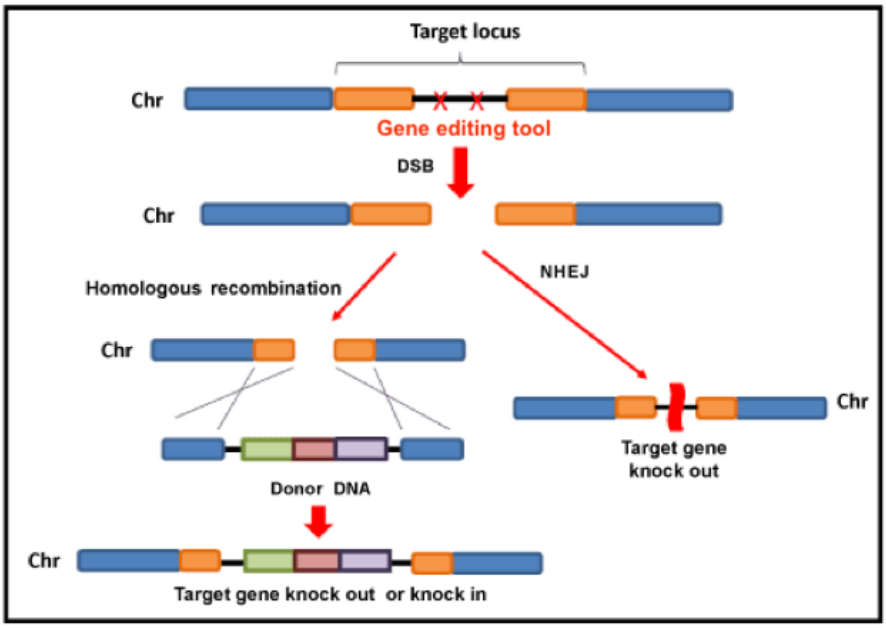

Figure 3. After the double-stand breaks, homologous recombination or non-homologous end joining could happen, depending on the stimuli provided by the culture environment.

Gene editing can be performed by meganuclease, Zinc finger, TALEN and CRISPR-Cas9, being the last enzyme the one used in this study.

1.2. Adenoviruses

With the development of recombinant technology, gene therapy has become a biomedical approach to the genetic disorders because of its ability to introduce a therapeutic gene in a vector, which can correct the abnormal DNA sequences of the target cells and, thus, to restore the normal production of the specific protein and the cellular function. Compared with other non-viral vectors, viral vectors are more efficient in editing DNA, although its safety has been considered the main drawback. But during the course of time, many researches were performed to reduce the toxicity of these vectors.

Among the main viral vectors, adenovirus is selected as the vector candidate since they are not integrative, which means that they do not change the genome of the host cells but only make them to produce the proteins of interest. With this property, they are appropriate for treatment that requires short-term transgene expression like cancer. The adenovirus can carry suicide gene with the goal of tumor cell apoptosis (De-Gui Wang, 2016).

Other features of adenovirus are going to be discussed and taken into account when a therapy is being designed. Adenovirus is the largest non-enveloped adenovirus that only has an icosahedral nucleocapsid enclosing a double stranded DNA molecule. There are five genera of adenoviruses (Atadenovirus, Aviadenovirus, Ichtadenovirus, Mastadenovirus and Siadenovirus), among which the Mastadenovirus includes a type species called human mastadenovirus C, which are able to transduce human cells. Moreover, these human adenoviruses are classified into 57 types and 7 different species (from A to G). But the vast variation of adenoviruses, the characteristics of serotype 2 (Ad2) and serotype 5 (Ad5) are the mostly studied, being the last one the type of vector used in this study.

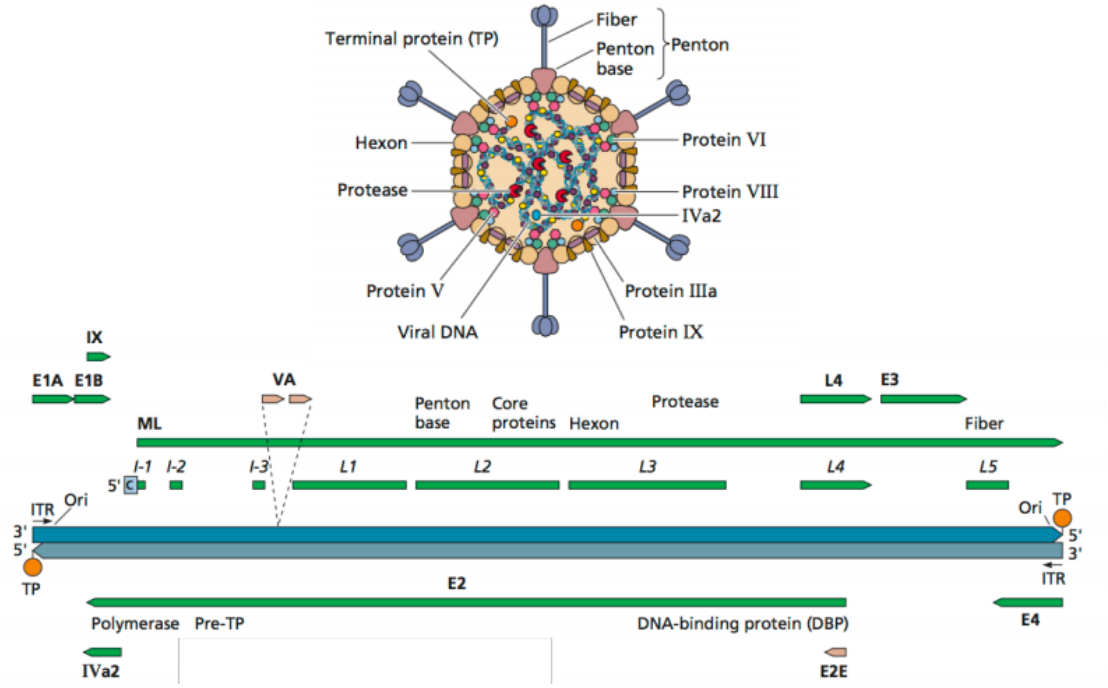

Figure 4. The genome and protein of adenovirus (Jane Flint, 2015)

The genome of adenovirus is about 36 kilobases and it can be divided in two different types according to their functions during replication. The regions E1A, E1B, E2, E3 and E4 are identified in the first part (Philip Ng, 1999) and illustrated in Figure 4. E1A proteins are involved in transcriptional regulation of the virus and stimulate the transduced cells to replicate, while the E1B inhibits apoptotic cell signaling. The E2 region is responsible for proteins necessary during replication, such as DNA-binding protein, viral DNA polymerase and terminal protein precursor. The E3 regions encodes proteins that evade the host immune system, so its lack does not affect virus growth in cell culture. The last region, E4, support the DNA replication by enhancing specific gene expression and decreasing host protein synthesis. The genes of the second part, numbered from L1 to L5, are expressed after viral replication to produce the viral capsid, that encompasses proteins such as fiber, penton base and hexon. The fiber of viral capsid binds to the coxsackie virus and adenoviral receptor (CAR) to attach to the host cell, then the penton base interacts with α_v integrin that initiates the endocytosis of virus. In addition to these two main viral proteins, there are others being found to play a role in adenovirus entry, like heparin sulfate proteoglycan. Once the virus escapes from the vesicle, it can reach the nucleus and form the capsid-nuclear pore complex in order to introduce the viral DNA into the host nucleus, as illustrated in Figure 5.

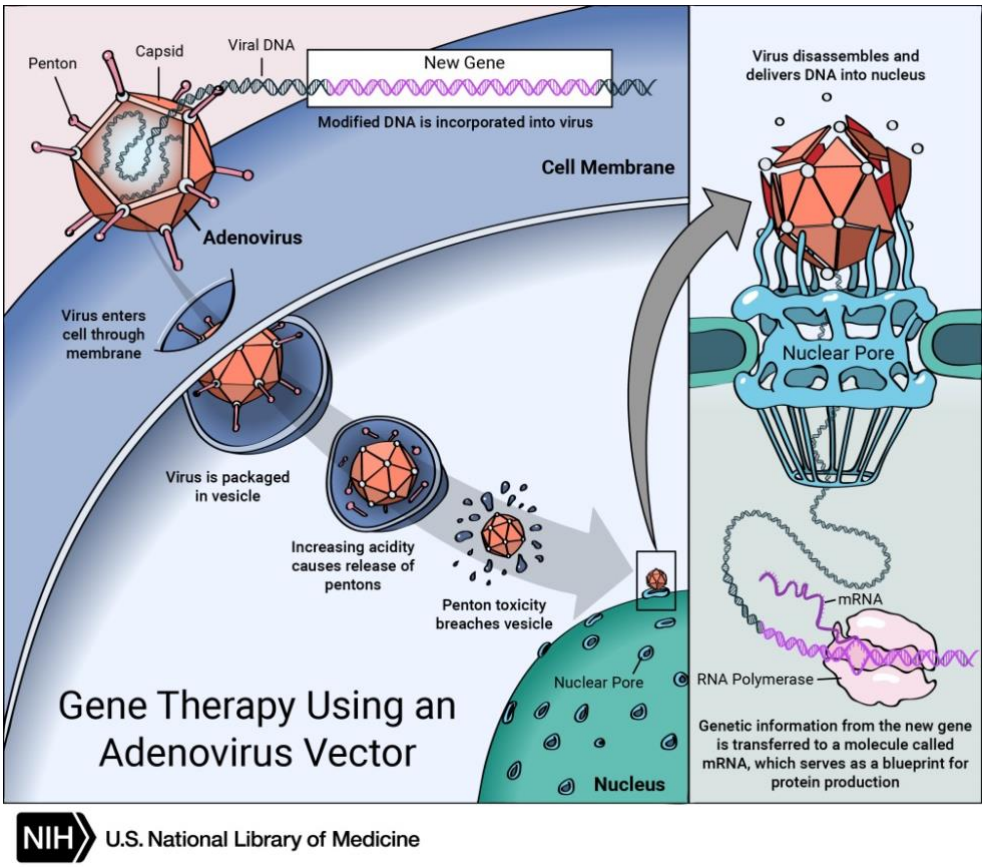

Figure 5. Adenoviral vector transduction. The adenovirus carrying the transgene enters the cell through endocytosis and escapes from the vesicle thanks to penton toxicity. Through capsid-pore complex, viral double strand DNA enters into the nucleus and can be expressed without being integrated into host-cell DNA (National Library of Medicine (US), 2013).

The extensive study about molecular mechanism of adenoviruses' genome and life cycle contributes to an easier molecular manipulation of their genome. Moreover, it is simple to package the whole genome because only the packaging signal (Ψ) and the inverted terminal repeat (ITR) are indispensable, both sketched in Figure 6. This implies that a large transgene cassette up to approximately 35kb can be introduced in the vector removing the rest of genome, permitting wide range of gene expressions. Additional benefits include the reliable virus production methods, high levels of expression in both replicating and non-replicating tissues.

However, there are also some drawbacks that limits their clinical application as vectors. A high dose of adenoviruses can be very toxic, because of the spread of viral protein and the activation of innate immunity. This was showed in 1999 with the tragedy of a patient participating in a clinical trial, during which $3.8x10^{13}$ adenovirus particles were delivered in an intravascular way through the hepatic artery. This *in vivo* gene therapy was designed to treat partial ornithine transcarbamylase (OTC) deficiency, a metabolic disease causing the accumulation of ammonia in the body. The adenoviral vectors were “E1-deleted”, E2A-temperature-sensitive carrying the normal OTC gene and targeting hepatocytes (Lehrman, 1999). As the administered dose was large, it caused first liver dysfunction and then many other organ failures, leading to the death of the patient.

This raised a huge concern about the safety of adenoviral vectors *in vivo* administration. Nowadays, investigators conclude several features that can increase adenoviral toxicity. The dose is extremely important, because when there are not enough adenoviral receptors in the host cells or tissue, these vectors will migrate to other organs, increasing the systemic toxicity. After this failure, the viral vector technologies were validated with stricter guideline. The innate immune response is another challenge. Serotype 5 adenoviruses are very common viruses in respiratory infection, so the patient may be previously infected with these cells and, therefore, deliver the specific antibodies. When they are administered again with adenoviral vectors, the innate system will quickly respond to it, stimulating a strong reaction.

In order to minimize the toxicity, a new generation of adenoviral vectors will be used: helper-dependent (HD) adenoviral vector.

1.3. Helper-dependent adenoviral vectors

These vectors are manipulated in such a way, that all its viral genes are deleted, except the inverted terminal repeats (ITRs) and the packaging signal (Ψ), which are in the cis-acting sequences necessary for the vectors to replicate and be packaged. A simplified viral genome sketch is found in Figure 6.

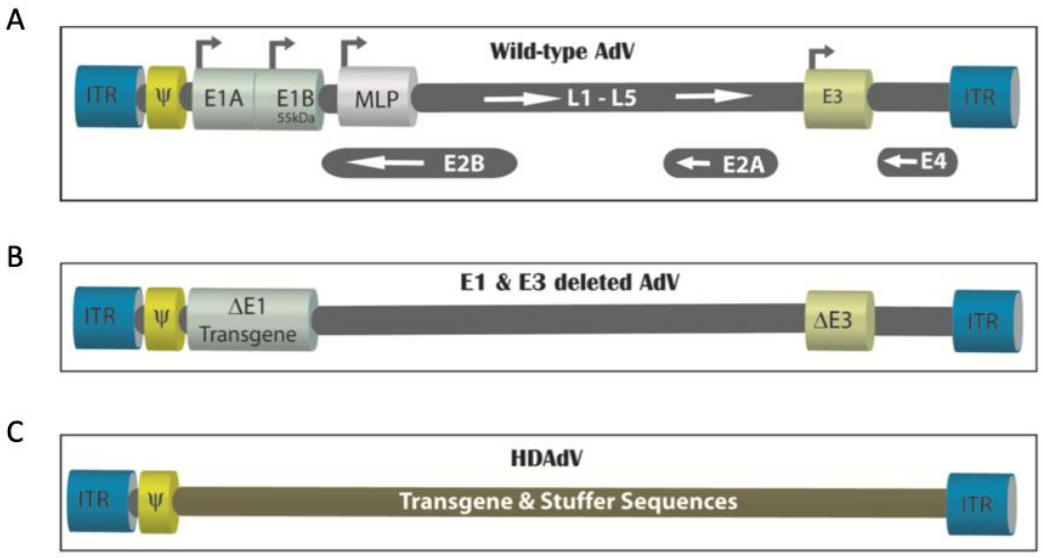

Figure 6. Serotype 5 adenovirus. A) Wild type Adenovirus. B) First generation vector, with deletion of E1 and E3, is replication-deficient. C) HD vector contains no viral gene except the ITR and Ψ. (Suresh K. Mittal, 2011)

With the deletion of almost all its genes, the vector can carry sequences about 35kb of length, which is relatively large and allow a lot of possible combinations. These combinations will yield a therapeutic effect in the host cells. In the case where the host gene editing is needed, the adenoviral HD vector can carry sequence encoding engineering nucleases, such as Transcription activator-like effector-based nuclease (TALEN) or (ZFNs) Zinc finger nucleases (Kim YG, 1996).

Since this generation of vectors cannot produce viral proteins, it depends on a second adenovirus, called helper adenovirus.

1.4. Helper adenoviral vectors

The genome of helper virus lacks fragment E1 while it retains the rest sequence necessary for growth and to support HD adenovirus packaging. Moreover, the packaging signal sequence of helper vector is flanked by two *lox*P sites. When helper viruses assist the HD virus production in 293 Cre4 cells, their packaging signal will be deleted. This is the key design to make possible that helper virus is only able to ensemble the viral genome of helper-dependent virus and with the presence of producer cells.

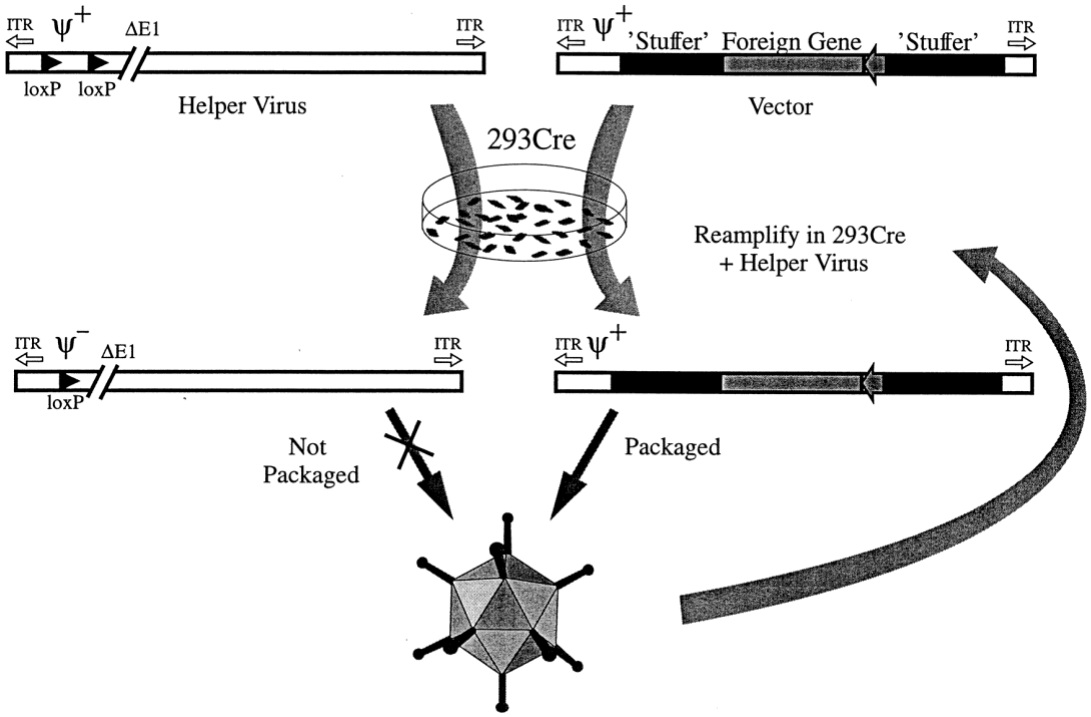

Figure 7. HD vectors packaging aided by Helper virus inside the 293 Cre4 cells (Robin J. Parks, 1996).

1.5. CRISPR-Cas9

CRISPR-Cas9 is a new genome editing tool with origin in bacterial adaptive immunity. The mechanism of CRISPR, cluster regularly interspaced short palindromic repeats, was discovered in 2007 by Barrangou and colleagues. When viruses or plasmids invade the bacteria, the foreign DNA is cut into small fragments and integrated into a CRISPR locus containing series of short repeats and localized near the Cas9 gene. After this locus is transcribed and processed, small RNAs (crRNA) are obtained. Once crRNA is associated with tracrRNA, they are able to guide the Cas9 that targets and cuts the complementary foreign DNA, as illustrated in Figure 8 A).

Basing on this CRISPR system, the trRNA and crRNA could be combined into a single guide RNA (sgRNA), as in Figure 8 B), in 2012 by Doudna and Charpentier labs(Jinek M, 2012). Compared with other engineered nucleases mentioned before, such as TALENs and ZFNs, Cas9 is simple to use because it does not need to generate a new nuclease pair for targeting each new sequence, which is a difficult and time-consuming process. By only reprogramming the two guide RNA, it can target any sequence.

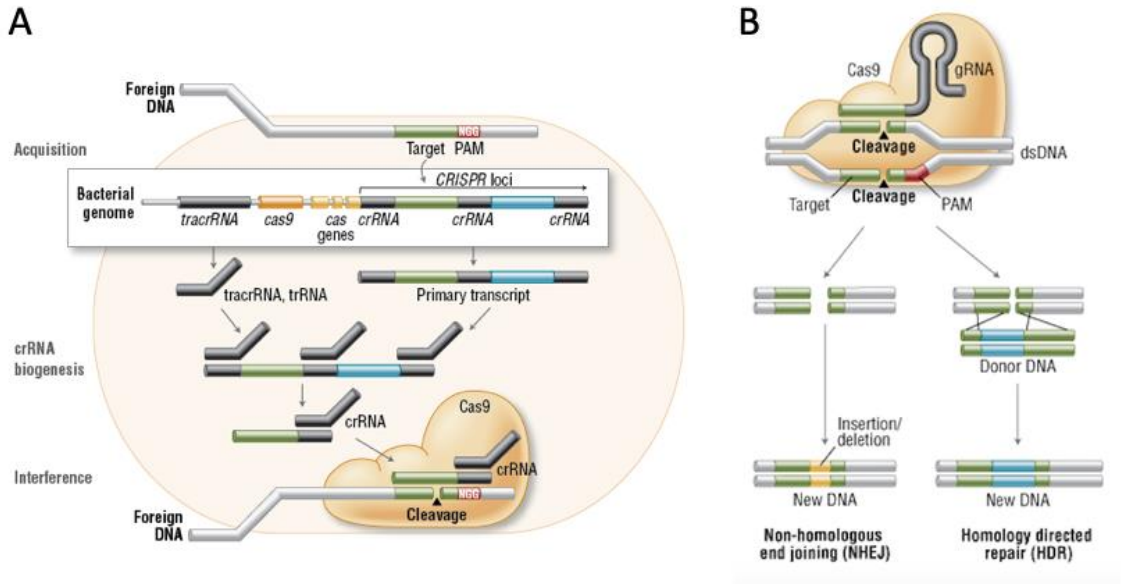

Figure 8. A) Cas9 activity in bacteria. Cas9 form a complex with both crRNA and tracrRNA in order to perform a site-specific DNA recognition and cleavage (Alex Reis, 2014). B) Engineered Cas9 activity. Once the Cas9 recognizes the PAM in the host cell and the sg RNA is complementary to it, cleavage will be proceeded.

This complex protein is mainly composed of two lobes, leaving a space to hold sgRNA between them during activation. In one of the lobe, the nuclease domains that actually break the DNA are found. They are RuvCs, HNH and CTD domains, being the last one containing sequence that will interact with the Protospacer Adjacent Motif (PAM). It should be recall that PAM and sgRNA are the ribonucleotides, such that they need to be recognized by the protein lobes at specific site to form the ribonucleoprotein.

Once the Cas9 complex becomes in contact to the DNA, it tries to target the sequence of interest. For that, it uses the PAM sequence to perform the first search. Once it finds the PAM, it denatures part of DNA and enables the base pairing of sgRNA and DNA. If they are totally complementary to each other, the DNA cleavage occurs. The wild-type Cas9 is able to create this DSB break, activating the repair mechanism that can be homology-directed repair (HDR) or non-homologous end joining (NHEJ), as illustrated in Figure 9 B). The problem of some types of Cas9 is that, a base mismatch can be tolerated, so that even they did not match perfectly, the protein can cut at wrong sites, a process called off-target activity (Lucas F. Ribeiro, 2018).

2. The skin

The structure of skin is important for a better understanding of the skin rare disease and the designed gene-editing correction. It consists of three layers, which are, from outermost to the innermost one, epidermis, dermis and hypodermis. Each of them is composed of different cells and proteins and performs a specific function.

2.1. Epidermis and basement membrane

It is epithelial tissue and is mainly compsed of keratinocytes, that derive from the basal layer (with cubical form) and migrate to the corneal layer (with squamous form), as illustrated in Figure 9. In this way, they are constantly being renewed. Between the corneal and basal layers, there are two more layers of cells between them. Beneath, there is a thin layer that connects it to the dermis, the dermal-epidermal junction (DEJ), a basement membrane. As any basement membrane, it consists of layers of extracellular matrix which are the basal lamina (lamina lucida and lamina densa) and the lamina reticularis, hold by attaching proteins such as collagen VII and fibrillin.

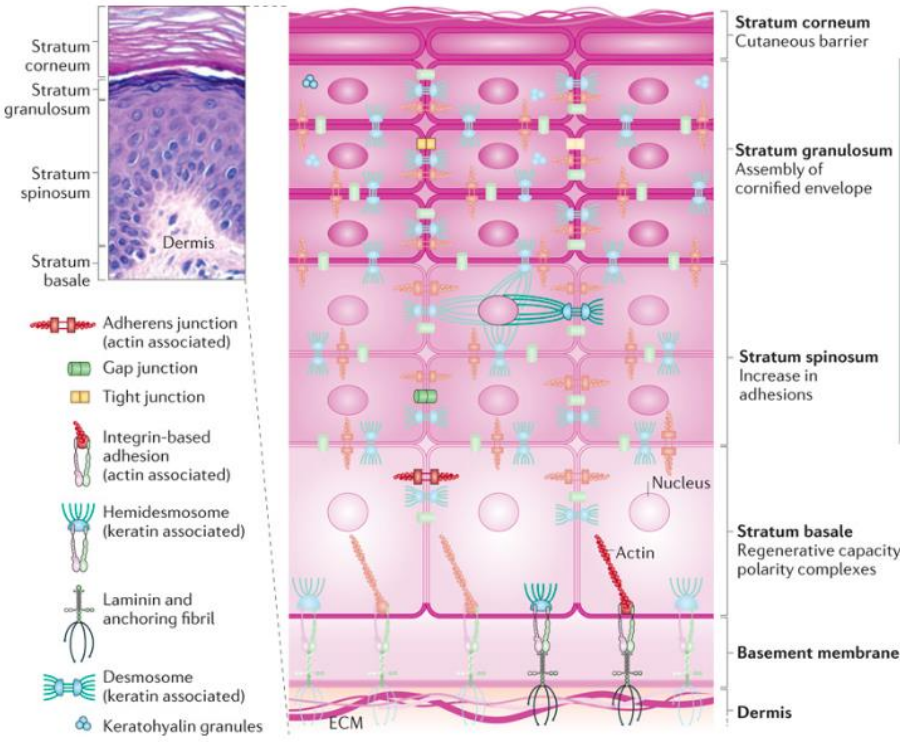

Figure 9. Main proteins in the epidermis with structural function (Lee, 2013).

In the dermoepidermal junction (DEJ), Collagen VII plays a crucial role because it attaches the lamina densa to the papillary dermis. Its malfunction or deficiency can lead to the separation of epidermis from the dermis even after a smooth rush, such that blisters form on all part of the body and leave scares.

2.2. Dermis

Rested beneath the DEJ, dermis is connective tissue that supports the epithelial tissue (epidermis) by providing the blood vessel, nerve and lymphatic vessels necessary for the proliferation and growth of keratinocytes.

It differs from the epidermis not only in the function because of different cell types and chemical compositions. In the upper tissue, the major cell type is keratinocyte, while in the lower tissue, it is fibroblast. This also induces the second difference: chemical composition. The epidermis hardly contains extracellular matrix except in the basement membrane, but the dermis is filled of extracellular matrix, synthesized by the fibroblasts.

Dermis also contains three layers, which are the papillary layer, the subpapillary layer and the reticular dermis, as in Figure 10. The top layer is attached to the basement membrane.

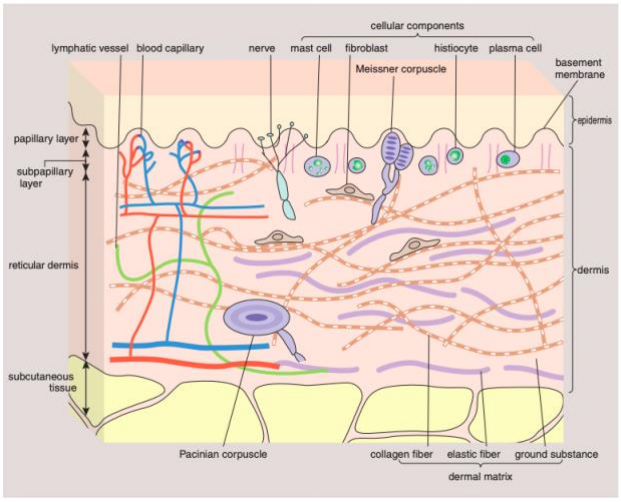

Figure 10. The structure of the dermis (Shimizu, 2007)

2.3. Hypodermis

It is the subcutaneous fat tissue that stores neutral fat and water, and that provides pressure resistance. The dermis is hold firmly to this deeper layer by fiber bundles called retinaculae cutis.

3. Dystrophic epidermolysis bullosa (DEB)

The dystrophic form of epidermolysis bullosa is a heritable skin disease characterized by abnormal blistering of the skin. This blistering can also occur on the mucous membrane and sensitive part like in the eyes. Depending on the phenotypes, it is classified in many groups, being the mildest phenotype the nail-only dominant DEB phenotype, while the most severe one is the severe generalized recessive DEB (RDEB). The last one can lead to large area of blistering and scarring causing the fusion of fingers and toes. But the deadly consequence of this phenotype is the development of squamous cell carcinoma, that occurs with a very high possibility.

From the genetic point of view, it is caused by mutation in the gene encoding the pro-alpha1 chain of type VII collagen (COL7A). This mutation can be inherited, being autosomal dominant or recessive. In order to understand how a mutation affects these proteins, we should first know the sequence at DNA level, then the resulting protein structure and function.

3.1. Collagen VII structure

The collagen type VII is the main protein of fibrils that tightly hold the epidermal basement membrane to the dermal layer. The mRNA of this gene consists of 8832 base pairs and contains 118 exons of short length that encode a polypeptide of 2944 amino acids. But the whole gene is about 31 kb on chromosome level. The gene contains a central domain made of Gly-X-Y repeat. This repeat, with a total length of 145 kD (approximately 220 bp), is responsible for the triplet helix formation and mechanical strength of the protein, but it is interrupted by 19 non-collagenous regions that provide flexibility to the long chain. There are some other non-collagenous domains that are important for collagen VII maturation and fibril formation. Every three chains of pro-alpha 1 twist to form procollagen helix molecules inside cells, as illustrated in Figure 11. Once they are secreted from the cells, they are processed and fold into a long mature collagen. Two Collagen VII monomers bind to each other in an antiparallel way and overlap in their carboxyl termini stabilizing disulfide bridges. Finally, to form the fibrils that tightly anchor the epidermal layer to the dermal one, lots antiparallel dimers stack together forming a single fibril.

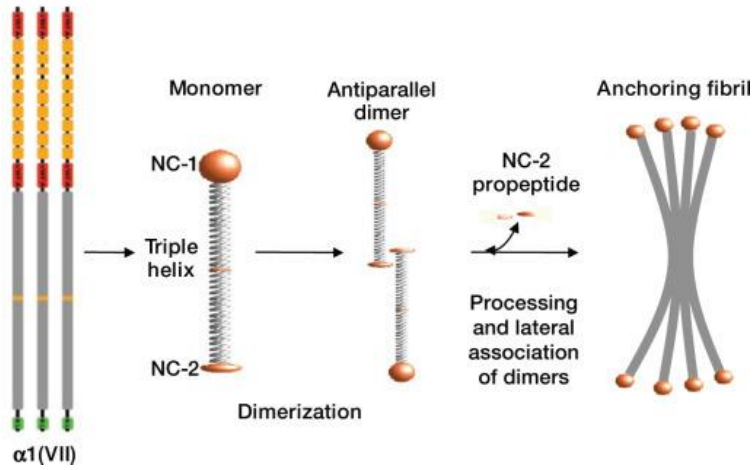

Figure 11. Collagen VII fibril assembly (Christelle Bonod-Bidaud, 2013)

3.2. Mutations in collagen VII coding gene

The genotype-phenotype correlation from a study (Peter C. van den Akker, 2011) shows that mutations, such as frame-shifting deletions or insertion, are the main cause of DEB. After the point of frame-shifting mutation, the reading frame shifts in such a way that the codons (each codon contains three bases) change completely and a premature stop codon can appear in DNA sequence or transcribed mRNA, resulting in a truncated and nonfunctional collagen product. The mutation leading a shorter transcript is called premature termination codon (PTC) mutation. This mutation can occur in one or both alleles. In mild DEB, there is normaly only one mutated allele, so that the amount of fibrils are reduced. In severe generalized DEB patients, the anchoring fibrils are absent in the skin because both alleles are mutated.

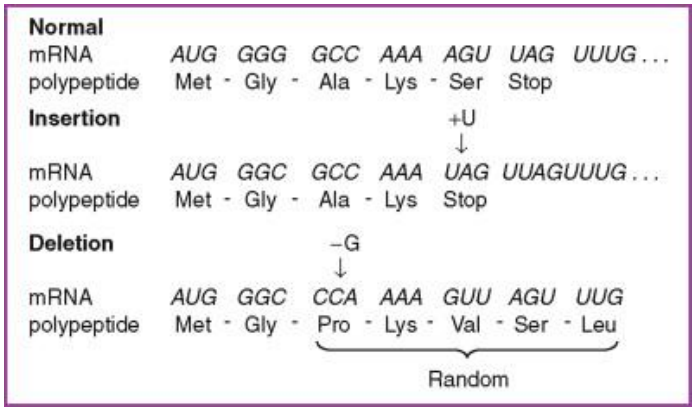

Figure 12. Insertion of Cytosine base at position 6527 causing frameshift mutation and yielding a different amino acids chain with shorter length (W.Pelley, 2012)

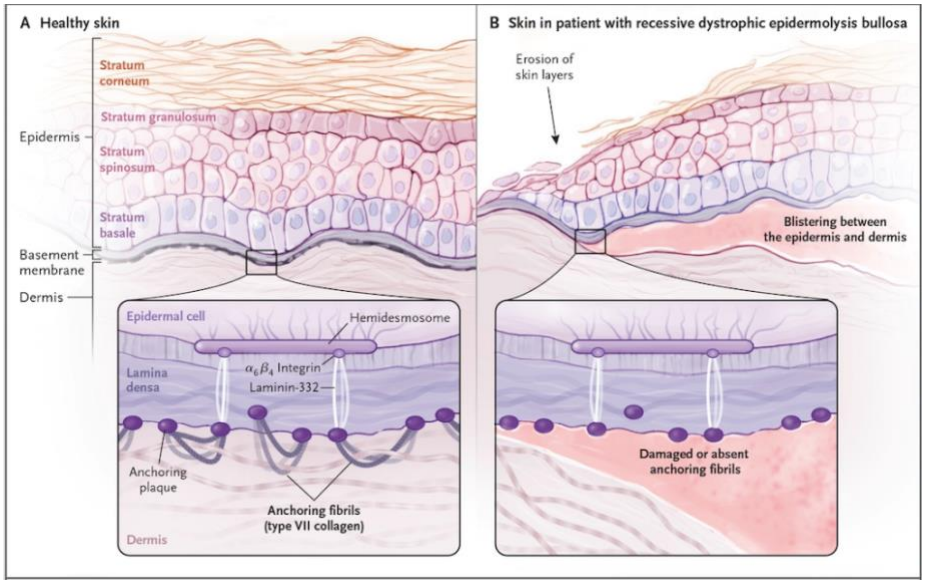

Figure 13. Simplified scheme of recessive dystrophic epidermolysis bullosa (Michael Vanden Oever, 2017).

3.3. Strategies for EB treatment

Many strategies have been designed in order to recover adhesion between dermis and epidermis through the recovery of the protein. Cellular therapy is one of the approaches. A good example is the European clinical trial based on the intravenous injection of normal mesenchymal stem cells (MSCs) collected from one of the parents of the RDEB patient (EudraCT Number: 2017-000606-37). It was showed that the MSCs extracted from bone marrow of a genetically similar healthy person were able to improve the *COL7A1* expression in the dermal-epidermal junction.

As the origin of the disease is caused by mutation, genetic therapy could restore the normal expression of the disease-causing gene for a longer period of time, without the need of several administrations. As illustrated in Figure 1, there is a high variety of methods. The non-viral approaches mainly use polymers or lipids to deliver the full length *COL7A1* (addition) (Cutlar L, 2016) or the gene encoding an engineered nuclease (gene editing).

Among the viral therapy, the lentivirus was firstly used to perform *COL7A1* gene delivery. Then retrovirus containing full-length *COL7A1* gene was able to transduce fibroblasts and correct the gene, thus corrected skin equivalent can be created and transplanted to RDEB patient. This autologous graft was tolerated during one year with collagen VII production (Georgiadis C, 2016; Georgiadis C, 2016).

Furthermore, the regeneration of the whole epidermis derived from corrected stem cells was achieved in a patient suffering junctional epidermolysis bullosa (JEB), another genetic skin disease characterized by the lack of laminin-332 in the basement membrane. The primary keratinocytes cultures were established from a small biopsy of a non-blistering area. After transduction with retroviral vectors expressing the laminin-332 gene, the transduced keratinocytes were cultured and expanded into epidermal grafts thanks to the presence of transgenic epidermal stem cells. Then they were transplanted on the dermal wound bed of the patient. Adhesion between the epidermis and dermis was still observed after 21 months of transplantation while no blister was formed in the regenerated epidermis (Tobias Hirsch, 2017). This approach is an *ex vivo* gene addition therapy approach.

All these advances strongly encouraged further gene therapy studies focused on genetic skin diseases.

MOTIVATION AND OBJECTIVES

Gene therapy is one of the most compromising treatment of a vast number of genetic disorders, that could not be treated with proper methods decades ago. With the technological advance and extensive basic researches, many of these diseases have been reported to be cured with gene therapy. Severe combined immune deficiency, hemophilia and leukemia are now target of clinical trials of this therapy. Furthermore, patient suffering metabolic disorders, neural diseases, and even cancer are now being treated with different kind of vectors. The gene modification is a such complex process that involves the entrance of vectors into the host cells, the delivery and expression of the genetic information that serves as a therapeutic purpose. The strategy strongly depends on the target cells and the type of vector used, such that every approach is specific and unique.

For epidermolysis bullosa, such as RDEB and JEB, long-term skin regeneration based on *ex vivo* gene addition therapy has been achieved with great results in the research center CIEMAT, but some problems were stated in this kind of therapy. The viral gene delivery efficiency is still low; the expression of the gene of interest cannot be accurately regulated to occur in the desired place and time; and the risk of insertional mutagenesis due to the usage of integrative viral vectors. Hence, gene correction was considered as a more precise alternative, in which the engineered nucleases perform site-specific cleavage in the mutated gene.

In a previous study (Cristina Chamorro, 2016), first-generation adenoviral vectors were used for correction of RDEB based on HDR and NHEJ. In Spain, the insertion of Cytosine base at positon 6527, within exon 80, (mutation c.6527insC) causes a recurrent frameshift mutation in 46% of recessive DEB alleles. Due to this high prevalence, the gene editing was focused on the exon 80. It showed that the deletion of exon 80 by using TALENS, delivered by adenoviral vectors, could restore the correct reading frame and subsequently, the collagen VII normal function in the adhesion between epidermis and dermis of skin.

The design and production of TALENS is tricky and time-consuming because the nucleases need to be modified according to the sequence of interest. For a generalized gene editing to treat many other mutations causing DEB, CRISPR-Cas9 system is considered a better tool. For this purpose, several dual sgRNA were tested to choose the sgRNA pair that results in the highest exon 80 deletion percentage. The ribonucleoprotein complex (sgRNA-Cas9) was delivered into the primary keratinocytes through nucleofection and was found to restore the reading frame of *COL7A1* in a large proportion of cells, which consequently synthesize functional collagen VII variant (Jose Bonafont, 2019).

Back to the delivery system for sgRNA-Cas9 complex, adenoviral vectors have been chosen because of their ability to infect quiescent cells like stem cells. But the first-generation is limited for *in vivo* application due to the relatively high toxicity due to the viral genome remaining in the host cells.

Therefore, this study aims at generating a less toxic version of adenoviral vector carrying a gene encoding sgRNA-Cas9 that can delete the specific exon and, in this manner, correct the collagen VII expression, as illustrated in Figure 14. For this purpose, simple 2D cultures are assessed in term of infection while more complex 3D cultures mimicking *in vivo* gene therapy are evaluated in DNA level to confirm the gene editing through NHEJ, following the workflow indicated in Figure 15.

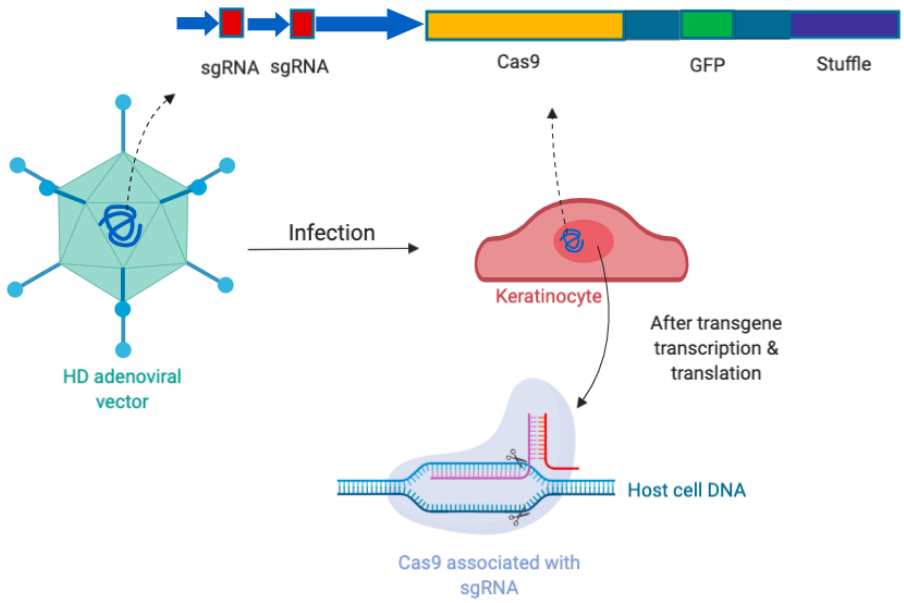

Figure 14. HD adenovirus serves as the delivery system of gene encoding sgRNA-Cas9 into the nucleus of infected keratinocytes Exon 80 skipping through sgRNA-Cas9 mediated cleavage followed by NHEJ.

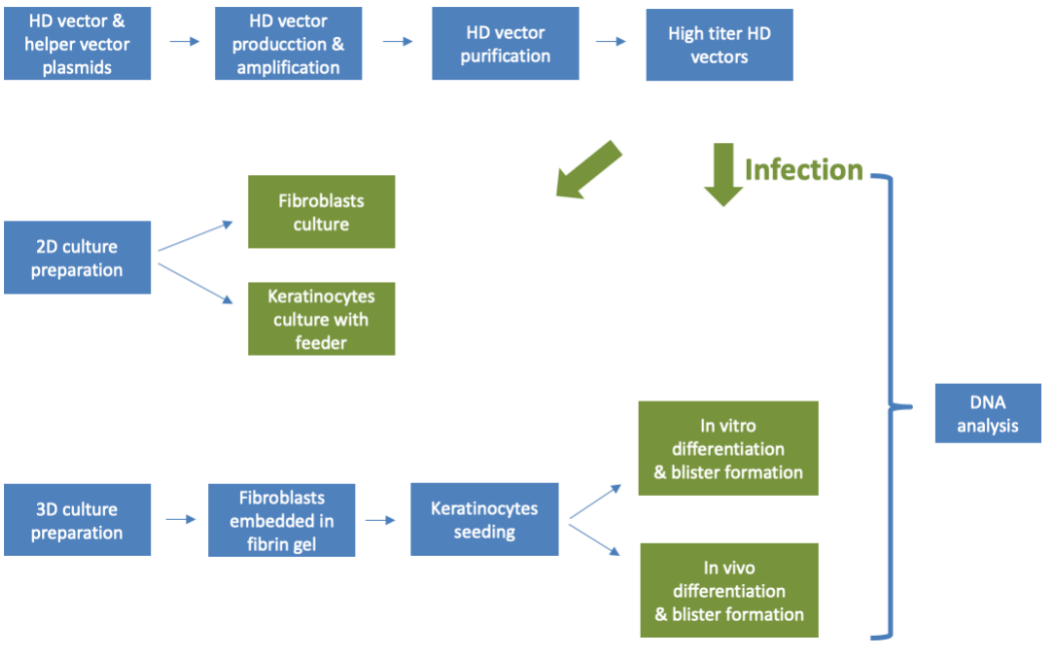

Figure 15. Simple workflow of the project.

MATERIALS AND METHODS

1. Patient primary cells acquisition

With informed consent and approval of the Hospital Ethics Committee, the human keratinocytes and fibroblasts with c.6527insC mutation in the exon 80 of gene *COL7A1* were extracted from a RDEB patient. After several cycles of mechanical disintegration and enzymatic digestion of the skin biopsies, the cells were extracted and cultured in conditions different for keratinocytes and fibroblasts or 293 Cre4 cells.

2. Culture of different cell types

All cellular cultures were maintained under a humid environment with 5% CO_2 concentration in an incubator (NAPCO) at 37ºC. To ensure a sterile condition, experimental work with cells was performed in laminar flow hood of biosecurity level II (BioUltra, Telstar®).

2.1. Keratinocytes

In normal physiological condition, keratinocytes rest on the layer formed by fibroblasts, which provide nutrients and signals through extracellular matrix to support the epithelial cells proliferation and differentiation. Nevertheless, the presence of fibroblasts makes the DNA analysis difficult, so alternatives to these cells, like feeder layer, were used. Feeder layer cells were modified in a way that they cannot divide, but still were able to provide extracellular secretions and support the proliferation of a single cell type culture. Depending on the type of target cells, feeder layer cells could be different, and for human keratinocytes, 3T3 cells could be used after being irradiated with a 50 Gy dose of X-Rays.

Keratinocytes seeding medium is used to promote cellular adhesion and consists of:

- 150 mL Dulbecco's Modified Eagle Medium (DMEM, GlutaMAX™, Gibco®)
- 75 mL of HAM's F-12 (F-12 Nutrient Mix, GlutaMAX™, Gibco®)) 2:1 proportion with DMEM
- 10% bovine calf serum (HyClone™)
- adenine (2.43 ng/mL, Sigma)
- cholera toxin (0.1 nM, Sigma)
- epidermal growth factor (10 ng/mL, Sigma)
- insulin (5 µg/mL, Sigma)
- Triiodothyronine (0.2 ng/mL, Sigma)
- antibiotics

After 48 h of incubation, seeding medium was replaced by the keratinocytes growth medium, which contains the same components as seeding medium but supplemented with 10 ng/mL epidermal growth factor (EGF, Sigma). This medium was renewed every 48-72 h.

When the culture reached a 90% confluency, subculture was proceeded.

The medium was removed firstly, followed by washing with Phosphate Buffer Saline (PBS, Sigma) and addition of trypsin for cell detachment. 20 minutes of incubation at 37ºC was needed to detach the keratinocytes. Once the cell detachment is confirmed through microscopic observation, trypsin is inhibited to avoid further digestion by adding DMEM.

2.2. Fibroblasts

Compared with keratinocytes, fibroblasts are more independent from other cell types. Moreover, medium used for seeding and maintenance has the same composition:

- DMEM
- 10% Fetal Bovine Serum (FBS, HyClone™)
- 1% antibiotics

For the subculture, trypsinization was proceeded, but fewer time was needed for fibroblasts detachment.

2.3. 293Cre4 cells

293 Cre4 cells are human embryonic kidney epithelial cells immortalized in laboratory. These cells were firstly obtained by being transduced with sheared adenovirus serotype 5 and, later they were selected because they could be maintained for several months. When the cells gradually adapted to tissue culture, they become a stable HEK cell line.

293 Cre4 cells are used in the propagation of adenoviral vectors since they play great role in the Cre/*lox*P method developed by Graham and co-workers (Chen L, 1996). Cre is a site-specific recombinase that acts on a target sequence called *lox*P. The pair of sequence *lox*P is found in the Helper virus genome, such that once the Helper vectors are cultured with 293 Cre4 cells, their DNA molecule will be cut at the Cre recombinase at sites of *lox*P, splitting into two fragments that cannot be packaged later, illustrated in Figure 7. This serves as a second restriction to avoid Helper virus from assembling their own genetic information and producing toxic viral protein.

Cryo-preserved 293 Cre4 cells were thawed in warm bath at 37ºC. They were counted before plating them and the concentration was calculated. To achieve a uniform distribution of cells, the dishes were covered firstly with culture medium, followed by the cell delivery.

As in the case of fibroblasts, the medium used for 293Cre4 cells seeding and maintenance has the same composition:

- DMEM
- 10% Fetal Bovine Serum (FBS, HyClone™)
- 1% antibiotics

3. Helper-Dependent adenoviral vector DNA construction

The generation of HD adenoviral vectors was based on the pC4HSU plasmid, that includes the adenoviral sequences necessary for vector DNA replication (Inverted Terminal Repeats, ITRs) and packaging, as well as non-coding human genomic DNA (stuffer DNA necessary to reach a minimum vector size). pC4HSU was digested with AscI and NotI restriction sites and ligated to a 6.3 kb BssII/ NotI fragment containing all the sgRNA-Cas9 system elements. This fragment was obtained from plasmid dg-PGK-SaCas9-iGFP, previously generated in the same laboratory for generation of first generation adenoviral vectors and includes a Cas9 and GFP expression cassette as well as two cassettes for expression of sgRNAs designed for generation of DNA breaks at sequences flanking *COL7A1* exon 80. The resulting plasmid, in which 4 kb of stuffer was replaced with the sgRNA-Cas9 elements, had a size of 37 kb, and was used for generation of the HD vectors.

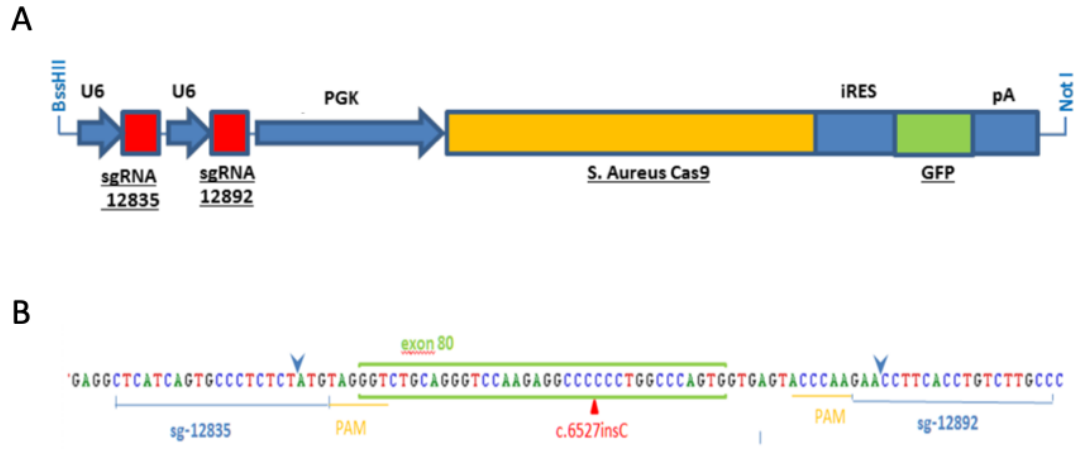

Figure 16. A) Transgene introduced into pC4HSU to express the sgRNA-Cas9 with two sgRNA and also to express GFP following a iRES. B) The two sgRNA target the fragments flancking the exon 80 and allow deletion by Cas9 at the site marked with blue arrows.

The PGK promoter drives Cas9 expression in all cell types, allowing the removal of DNA following the direction of guide RNAs. The Cas9 (CRISPR associated protein 9) used is a nuclease isolated from bacteria Staphylococcus Aureus, because this species of bacteria provides a Cas9 with a smaller size, such that it could be packaged into viral vectors more easily than other Cas9 variants derived from bacteria, such as the widely used Cas9 from Streptococcus pyogenes. Moreover, S. aureus Cas9 is more specific in term of PAM requirement (S aureus PAM is more complex and less frequent in the human genome than S pyogenes PAM), minimizing possible wrong targeting.

SgRNA (single guide RNA) 12835 and 12892 carried by the transgene are small RNAs, complementary to two DNA sequences of 20 bp flanking the fragment to be deleted (*COL7A1* exon 80). The numbers 12835 and 12892 specify the position of the guide RNAs and correspond to numbers in a DNA fragment that contains the *COL7A1* gene.

IRES is an RNA sequence that initiates the translation of GFP downstream sgRNA-Cas9. In this way, Cas9 and GFP are co-expressed and therefore the cells expressing sgRNA-Cas9 are detectable by fluorescence microscopy. The PAM sequence (Protospacer Adjacent Motif) is the genomic sequence immediately adjacent to the sequence complementary to the guide RNAs and its presence is necessary forCas9 RNPs functionality.

Plasmid subcloning for generation of the final HD construct was done using XLBLUE competent cells. For each subcloning step, miniprep plasmid DNA was analyzed by restriction analysis to check the construct content.

4. HD adenoviral vectors production

4.1. Viruses preparation for the transfection

One day before transfection, HD vector was linearized by digesting 5 µg of plasmid with PmeI restriction enzyme for 2 hours and then heating to 65ºC for 20 minutes. Then it was purified by Phenol/Choloroform extraction and ethanol precipitation and after resuspension in TE (Tris-EDTA) buffer it was stored at 4ºC for the transfection. One hour prior to transfection, the culture medium was replaced by freshly prepared medium without washing.

To set up the transfection reaction, herring sperm DNA at a concentration 1100µg/mL was added to 1mL of HBS (HEPES-Buffered Saline) buffer in a polystyrene tube. The solution was vortexed for 1 minute at maximum setting. Then the HD vector plasmids was added to the tube and mixed gently. 25µL of 2.5M CaCl2 were added dropwise with mixing and the whole solution was incubated at room temperature for 30 minutes.

4.2. 293 Cre4 cells transfection

0.5 mL of the prepared solution was applied dropwise to the monolayer of 293Cre4 cells and the dish was rocked to distribute the precipitate uniformly. Then overnight incubation proceeded.

The next day, the medium was removed from the transfected monolayer (with HD vectors), that was later washed with DMEM and then immediately transduced with helper virus at a multiplicity of transduction (MOI) of 5 pfu/cells. There were $3x10^6$ cells in the dish to be transduced, so we needed 3 µL of Helper virus with concentration of 10^9 particles/200 µL to achieve MOI of 5 pfu/cells. The Helper virus was adsorbed for one hour in the incubator with rocking every 10-15 minutes. Then 5 mL of DMEM was added to the monolayer.

Complete cytopathic effect (CPE), which means more than 90% of the cells are rounded up and detached from the dish, was observed by about 48 hours post-transduction. At this time, the cells were scraped into the medium and the whole cell suspension was transferred into a polypropylene tube and then stored at -70ºC after the addition of 10% volume (around 5mL) of 40% sucrose.

4.3. Serial passages

The frozen first passage lysate was thawed at 37ºC, at which condition the 298 Cre4 cells break, and 0.4 mL of lysate was taken to transduce a 60-mm dish of 90% confluent producer cells at MOI of 1 pfu/cell, then the monolayer was transduced with 0.4 mL of helper virus. The dish was returned to the incubator for one hour of adsorption, followed by the addition of 5 mL maintenance medium.

After observing complete cytopathic effect through microscope 48 hours after transduction, the cells were resuspended in the medium by scraping them, and transferred to a new polypropylene tube. This second passage of the vector was again stored at -70ºC after the addition of 0.5 mL of 40% sucrose.

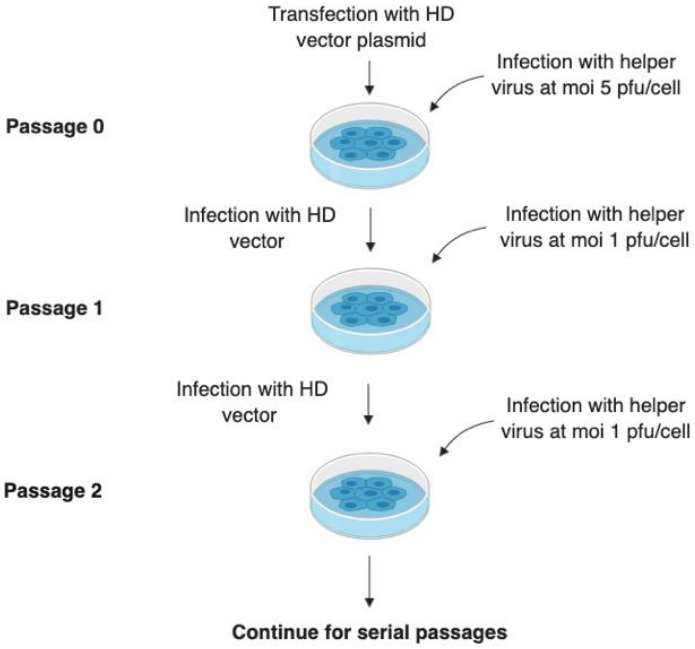

Figure 17. Overview of the protocol for production of the HD vector by serial coinfection with helper virus.

4.4. Amplification

After seven serial passages, the latest passage was chosen for large-scale preparation of HD vector.

Twenty dishes of 150 mm diameter were seeded with 0.5 million of 293Cre4 cells each. One week later, when 90% confluency of the producer cells was observed, 1 mL of Helper Dependent vectors and 1 mL of Helper vectors were added to each dish to coinfect the cells at a MOI of 1 particle/cell. The dishes were rocked every 10 to 15 minutes in order to ensure uniform interaction of vectors with the cells and were placed in incubator for one hour, process completed with the addition of 15 mL of DMEM to each dish.

Complete CPE was observed 48 hours post-transduction, so the cells were scraped into the medium and the cell suspension was collected for extraction purification of the HD vector.

5. HD adenoviral vectors purification

5.1. HD vector extraction

The harvested cells and medium underwent centrifugation. The supernatant was discarded and the cell pellet was resuspended. Then it was centrifuged again at 4000 rpm for 10 minutes to separate the cellular and viral components. This time the supernatant was collected while the pellet containing cellular debris was discarded.

5.2. CsCl step gradient preparation

CsCl centrifugation, used for density-based separation, is a process in which the molecules to be separated are mixed with CsCl and centrifuged at very high speeds overnight. The gradient consisted of overlays of CsCl of different concentrations. 0.5 mL of 1.5g/mL CsCl solution was firstly added, then 3 mL of 1.35 g/mL solution was overlaid, following by overlaying 3 mL of 1.25 g/mL solution. Then 5 mL of supernatant containing the viral vectors was applied to the top of the gradient. Finally, the tubes were topped up with 100mM Tris-HCl.

5.3. CsCl centrifugation

The tubes were spun at 35000 rpm overnight. The centrifugal force caused the components of the mixture to separate by size and gradually pushes the components with higher density toward the bottom of the tube. The centrifuged solution contained several bands corresponding to viral vectors separated by density, being the band at the bottom denser than the band at the top. The genome of Helper vectors is slightly larger than that of HD vectors, and therefor the bottom band corresponds to the Helper and the top band to the HD vector.

The top band was collected with needle and syringe by piercing the side of the tube, taking as much of the band as possible. Then it was transferred to Slide-A-Lyzer dialysis cassettes that had been previously submerged in distilled water to remove the glycerol. Then the cassettes were submerged into 500 mL 10mM Tris-HCl and spun overnight, with two changes of the same solution. In this way, the salts of CsCl were removed from the vectors.

Figure 18. Viral band obtained after CsCl ultracentrifugation.

The titer of the viral vector preparations was determined by spectrophotometry. The concentration of viral vectors is directly proportional to the concentration of viral genomic DNA. The purified virus particles were diluted 20-fold with Tris-HCl/0.1%SDS buffer. Then the virus sample was measured at A_{260} with the NanoDrop and the concentration is calculated by using the following formula:

$$\mathrm{OD260} \times \text{Dilution Factor} \times 1.1 \times 10^{12} \times \frac{36}{Vector\ Size}$$

6. 2D culture preparation and transduction

After reaching 90% confluency, they were infected with HD adenoviral vectors at different MOI.

6 days after infection, the cultures were observed through fluorescence and brightfield microscopy, while images were acquired for analysis.

Both the brightfield and fluorescence microscopy images were obtained 6 days after the transduction. Due to the different texture, brightfield images were processed by following part of a protocol (Čepa, 2018), while the fluorescence images were processed in a different method. To begin with, they had to be converted into 8-bit grayscale images.

1. Brightfield image enhancement through histogram equalization: run (“Enhance Contrast…”, “Saturated=0.3%”, “equalize”)

2. Canny edge detection with Gaussian Kernel: run ("Canny Edge Detector plugin”, “Radius=1”, “Low threshold=4”, “High threshold 7.5”, “Normalized contrast”)

4. Closing, a morphological operator that fills the remained small holes

5. Dilation, another morphological operator that expands the shapes after closing

For the fluorescence images, due to their smooth texture, the processing steps simply consisted of thresholding with a range of 23 to 255 intensity, followed by dilation.

Now, the image contained maximum value in the background (white) and minimum value in the positions representing the cells. Area fraction (Analyze>set measurement) was used to assess the confluency percentage and the percentage of transduced cells (with respect to the whole image). The percentage of transduction with respect to the existing cells was calculated by using the following formula:

$$\%\text{transduction} = \frac{B}{A} \times 100$$

In which *A* is total cell area and *B* is the fluorescent area of cells transduced with the adenoviral vectors.

7. 3D culture preparation and transduction

7.1. Skin equivalent preparation

This culture system mainly consisted of two cellular components: keratinocytes and fibroblasts, maintained in differentiation medium and fibrinogen respectively. The keratinocytes were the same used in 2D culture, while the fibrinogen was obtained from pig blood plasm in the form of cryoprecipitate. Fibrinogen was found in liquid state at room temperature but it would form gel in the presence of thrombin, which in turn, would need calcium to be activated. Calcium had its origin in CaCl2 solution. Another detail of the mixture was the addition of tranexamic acid that avoided the degradation of fibrin by fibrinolytic enzymes called plasmin. In the lab, the plasma was not viscous on its own, but when it was in contact with fibroblasts, these cells speeded up the gelling process of plasma due to the presence of proteins involved in pre-inflammatory condition.

The key step during fibroblasts seeding was to achieve a homogenous distribution of these cells within fibrinogen solution and to prevent the gel formation inside pipettes that makes the seeding difficult. For this purpose, fibroblasts suspended in human keratinocytes medium were mixed with tranexamic acid, proteinase and thrombin solution while the cryoprecipitate component was introduced in the last moment to complete the mixture. The manipulation was fast to avoid gel formation inside the pipette.

In each well, there was a mixture of 3.5 mL containing the following:

- 100K fibroblasts resuspended in human keratinocyte medium
- 60 µL of tranexamic acid
- 500µL of a 0.025mM CaCl2 (Sigma Aldrich) dilution in which11 IU of thrombin (Sigma Aldrich) is found
- 1mL of blood cryoprecipitate (fibrinogen)

Two different plates were used and later incubated at 37ºC in a 5% CO2 atmosphere to allow the fibrin gel formation. The first one contains transwells, the function of which was to allow the air-liquid interface, the main mechanism of keratinocytes differentiation *in vitro*. The other plate with normal wells would be used for engraftment on mice.

Once the fibrin gel was formed, primary keratinocytes were thawed in warm bath, and then resuspended in the differentiation cocktail described in section 2.1., but with 1% bovine calf serum instead of 10% and ascorbic acid (50 µg/mL).

To the two organotypic culture plates where the blister would be created artificially (*in vitro*) and to one plate of culture prepared for transplant (*in vivo*), $5x10^5$ normal keratinocytes suspended in the seeding medium were seeded directly on the solidified fibrin gel.

7.2. Keratinocytes differentiation

7.2.A. *In vitro* differentiation and maturation

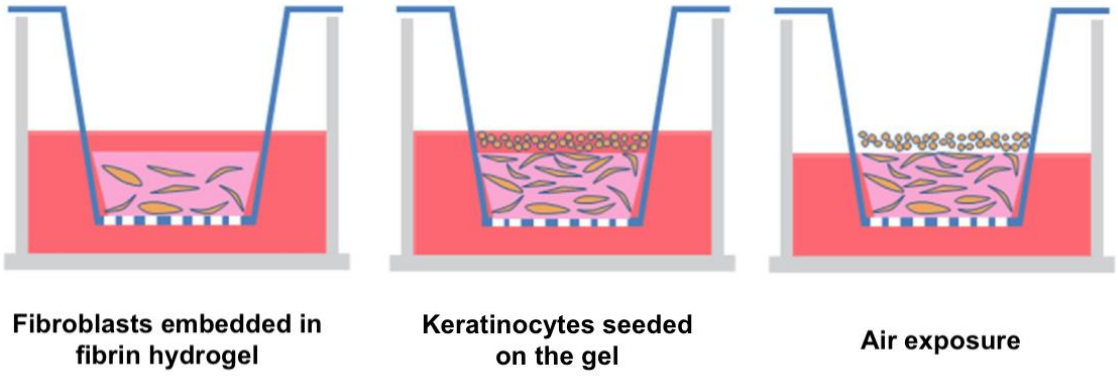

Figure 19. *In vitro* differentiation of keratinocytes due to the air-liquid interphase and differentiation medium.

The differentiation was stimulated by the change in the composition of the culture medium and also by the air-liquid interface that assembled to the real biological environment of skin. The outermost layer of skin was always exposed to air while the basal part rest on the dermis. Therefore, in order to differentiate the keratinocytes into squamous stratified tissue, the basal part of these cells had to be in contact with the medium. In this way, the keratinocytes proliferated, gradually left the medium and became in contact with the air, in a way that they differentiated following this gradient. At the same time, the dermal layer was always immersed in maintenance medium. This was the most commonly used approach for *in vitro* 3D skin model and the whole process of differentiation of keratinocytes and epithelium formation takes 20 days.

7.2.B. *In vivo* differentiation and maturation

Once the seeded keratinocytes reached confluency and completely attached to the fibrin matrix, the whole structure was separated from the culture plate for transplantation on immunodeficient mice. According to the methodology described in (MARCELA DEL RIO, 2002), a 20-mm circular partial-thickness fragment (containing epidermal and dermal layers) on the mice dorsum was removed from the skin and underwent devitalization through three repeated cycles of freezing and thawing. This process turned this removed piece of skin into a biological bandage that, after being sutured on the skin, held and protected the organotypic placed on top of the wound area.

7.3. Blister formation and adenoviral vectors injection

Blisters were created on organotypic cultures to mimic epidermal-dermal detachment in RDEB and allow the evaluation of different viral vectors to deliver gene-correcting molecular tools. This assessment was performed both *in vitro* and *in vivo* conditions.

7.3.A. *In vitro* condition

After 7 days of differentiation through air-liquid interface *in vitro*, the epidermal layer acquired different properties and phenotype than dermal layer, such that two layers could be easily identified after one week of incubation. This difference facilitated the whole process. The blister was formed by using a syringe with needle. Firstly, the needle was inserted beneath the upper layer, then air was injected separating a little bit the two layers.

7.3.B. *In vivo* condition

Compared with *in vitro* differentiation, *in vivo* condition provided a better environment for the organotypic culture to mature and become more similar to natural skin tissues. As this regenerated skin was tightly attached to the mouse hypodermis and the different layers could not be distinguished, the method used in the *in vitro* section was not suitable. An alternative needed to be used for blister formation.

The mouse was anesthetized and prepared for manipulation. The first step was to check the autofluorescence of normal living cells in order to obtain a reference image allowing later observation of fluorescence emitted by the transduced cells. The area of graft was then marked for easier visualization during the whole process. The second step consisted of the device setup. The cylindrical plastic chamber was placed on its dorsum, in such a way that the human skin graft just matched the hole of the chamber. The chamber was connected to the vacuum generator. Once the pressure supply was turned on, the compressed air was accelerated and generated a suction effect. The appropriate pressure range spanned from 10inHg to 13inHg (254 to 330.2mmHg). The skin should be carefully stretched, so that only the graft was under suction, otherwise the blister would not form between the epidermis and dermis.

After obtaining the blister, the aliquots of adenoviral vectors were firstly mixed with 30mL of Matrigel, and then injected inside the blistered graft. The Matrigel solution, containing mainly laminin and collagen, prevented viral suspension from leaking out from the blister. In this way, fibroblasts and keratinocytes could be infected with as many viral particles as possible. Finally, the light from the device promoted the polymer gelation by heating it.

8. DNA extraction, amplification and analysis

8.1. DNA extraction

Keratinocytes or fibroblasts maintained in 2D culture were collected and centrifuged to remove the medium. Then, they were distributed to different 1.5 mL tubes, according to the MOI, to be processed. However, in 3D culture, the epidermal and dermal layers must be separated and processed in two tubes respectively for each MOI.

The following tissue digestion protocol was common for both culture systems. The first step was the addition 700 µL of lysis buffer with the following components:

- 20 µL of 50mM Tris-ClH (pH 8)
- 80 µL of 100mM EDTA (pH 8)
- 8µL of 100mM NaCl
- 40 µL of 1% SDS

Then 18 µL of proteinase K (20mg/mL) was added to digest the proteins.

After overnight incubation at 55ºC at 650 rpm, 4 µL of RNAase A+T1 was added and followed by 30 minutes incubation at room temperature. Then 250µL of saturated NaCl was added and the tubes were shaken for 10 minutes without using vortex. After 5 minutes of centrifugation at 14K rpm, 850 µL of supernatant containing DNA was collected to another tube. 500 µL of cold Isopropanol was used to precipitate DNA molecules when the tubes were being smoothly shaken for 5 minutes, followed by 5 minutes of centrifugation at 12000 rpm. After removing isopropanol, 500 µL of 80%ethanol was applied to wash the pellet for 3 minutes of centrifugation at 12000 rpm. Ethanol was removed as much as possible but ensuring intact DNA pellet. Finally, DNA molecules was dried at 37ºC and stored in water for later PCR (Polymerase Chain Reaction).

8.2. Polymerase Chain Reaction

The concentration (ng/µL) of extracted DNA was confirmed by using spectrophotometer (ND-1000, NanoDrop), and PCR genotyping was performed in the following conditions

- 1.5 µL of 10x Buffer
- 1.5 µL of MgCl2 (25mM)
- 2 µL of dNTPS (10mM)
- 1 µL of primer targeting *COL7A* R [10] (5’ -ACCCCACCAAGGAAACTGA-) (10mM)
- 1 µL of primer targeting *COL7A* F1 [10] (5’ -GTGAGTGGTGGCTGAAGCAC-) (10mM)
- 6.35 µL distilled water
- 0.15 µL of Taq Polymerase enzyme (5 units/µL, Invitrogen)

The PCR program was:

Stage	Repeat time	Temperature (ºC)	Time (second)
1	1	96	300
2	5	96	30
		65	30
		72	30
3	30	96	30
		60	30

8.3. Agarose electrophoresis gel

The fragment amplified by PCR contained the intron 79 and exon 80 while the segment removed by Cas9 consisted of exon 80 and some adjacent base pairs, such that a total deletion of 57bp was expected. In order to visualize the deletion of this small segment, 1.5% (1.5 g/100mL solvent) of agarose gel was prepared. (Technology for Genetic Analysis, 2012).

First of all, low EEO agarose powder (CONDA) was weighted and dissolved in corresponding volume of 10X TAE or TBE 1X, after being boiled and shaken. The bottle was cooled a little bit and ethidium bromide was added with 0.005% (volume) to interact with DNA and to make it visible under UV light. Then it was poured into the plate mold and the wells were created by inserting a comb into the slots, and let it solidify at room temperature. Once the gel was totally solid, it was placed in the electrophoresis box. The chamber was filled with the same solution in which the gel was made of (TAE 10X or TBE 1x).

Then 5 µL of molecular weight marker ladder was pipetted into the leftmost well. The ladder called IX was mostly used. These PCR molecular weight markers contained smaller DNA fragments than normal DNA markers and depend on the type of marker used, different ranges of size could be determined, being the number of base pairs directly proportional to the molecular weight (1 base pair=660 Daltons). Marker IX (Sigma) contained 11 DNA segments with increasing length starting from 72 bp while ending in 1353 bp, which were determined by computer analysis of DNA sequence. A mixture of 5µL samples and dye was loaded. The electrophoresis box was set at 100 volts

8.4. Cas9 nuclease protein activity

Once the image was acquired through the imaging device (ChemiDoc™ MP Imaging System) and saved in format tif., the intensity of the bands was quantified using ImageJ program.

Following a tutorial (lukemiller.org, 2010), the tool, *Gel Analyzer* was used. Firstly, the RGB images were converted into gray scale image (8-bits), then different lanes with the deletion lanes were selected.

With *Plot Lanes*, the profile of each lane represents the relative density of the contents of the band over each lane. The bands arranged vertically (top to bottom) is localized from the left to the right in the plot. The higher and wider the peaks are, the darker and wider the bands are. As there was noise in the background of the blot, the values did not reach zero at the end, such that the profile remained open. In order to calculate the area (integral), a *line* was drawn manually while another line was used to separate the two bands as showed in Figure 20. Then by using *Wand Tool*, different areas representing different bands are selected and analyzed in term of area. Through *Label Peaks* the percentage was obtained through following formula:

$$\%\text{Area} = \frac{b}{a+b} \times 100$$

in which *a* is the integral of the intensity of the band representing to the intact DNA segments, while *b* is the integral of the band corresponding to the corrected DNA segments.

Therefore, the percentage of area of the bottom band is the deletion percentage.

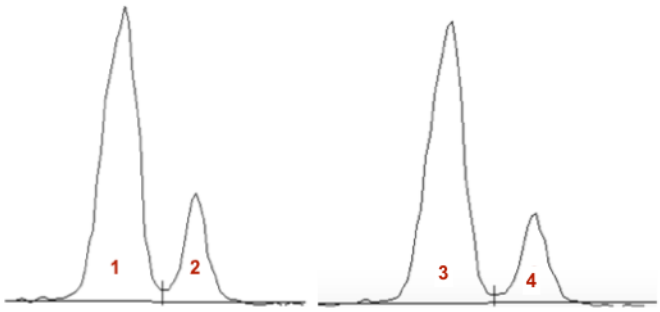

Figure 20. A) As an example, the plot obtained from the Plot Lanes of the PCR bands of dermis infected with HD Ad (1 and 3 are top bands while 2 and 4 are bottom bands). Lines were drawn to separate the bands and calculate the integral (area).

9. Toxicity assessment

9.1. DAPI staining of keratinocytes

Keratinocyte cultures were prepared following the same procedure described in the section 4.1., and transduced with HD or first generation adenoviral vectors. At day 6 of transduction, the cells were stained with DAPI (4′,6-diamidino-2-phenylindole) solution (10µg/mL). The membrane of dead cells tends to be porous and, therefore, more permeable to the staining than the living cells. Based on this fluorescent stain, living cells could be differentiated from the dead cells through flow cytometry.

Firstly, the cell suspension was centrifuged to be collected in form of pellet. Then the DAPI stock solution was diluted in staining buffer. 1 mL diluted volume was added to each cell sample, followed by incubation of 15 minutes at RT.

9.2. FACS analysis

The stained cell samples were analyzed by using FACS (fluorescence-activated cell sorting), a type of flow cytometer. The FACS device excites the sample by using a UV laser and detects the fluorescent light emitted by the DAPI inside cells responding the stimulation. Then it classifies the cells according to a set threshold of emission intensity, so that cells with intensity higher than this threshold are sorted as dead cells while those with lower intensity are considered living cells.

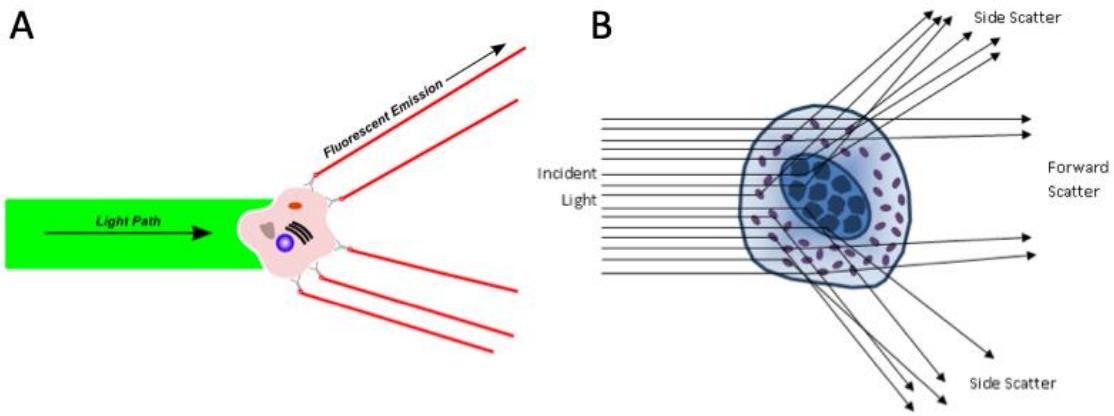

Figure 21. A) How the stain emits fluorescent light in response to the light excitement. B) How the incident light is reflected.

In the case of DAPI FACS, the fluorescent light was emitted from the nucleus. The forward scatter measured the size of cells by basing on the light diffraction around the cell. Cells with larger diameter have higher FSC intensity. Side scatter measurement could reveal the cell internal complexity.

RESULTS

1. Serial passage and HD adenoviral vector concentration

The construct was designed in such a way that it expressed specific guides and Cas9 protein inside the host cells to restore the COL7 production by eliminating the exon 80. For that purpose, once the 293Cre4 producer cells were transduced with Helper-Dependent vectors and then with helper vectors, the virus production started. As a GFP sequence was connected to sgRNA-Cas9 with iRES between them, the cells that expressed this green fluorescence protein could be identified with microscope. The increase in intensity and number of fluorescent cells also showed that they produce more viral vectors during each passage illustrated in Figure 18.

Living 293Cre4 cells were normally found attached to the bottom of culture plate while the dead ones were floating, such that the cell viability could also be checked through live cell imaging. The perfect passage to be amplified was defined as the culture with as much viral vectors as possible inside living Cre4 cells, that protected the viral particles from being discarded through cells collection and centrifugation.

After amplification and collection through CsCl gradient ultracentrifugation to remove the toxic Helper vectors and other cellular components and to concentrate the vectors, Slide-A-Lyzer dialysis was carried out to complete the purification. A concentration of $8x10^{12}$ particles/mL is obtained with vector size of 37kb, dilution factor of 20 and OD_{260} of 0.374.

This concentration is used to calculate the particles applied to the cell cultures in order to achieve certain MOI for later gene editing efficiency assessment. It does not always hold, that the higher the MOI is, the better results are obtained, because a large number of viral particles can be toxic.

2. 2D culture gene editing

Keratinocytes synthesize two third of collagen type VII in skin while fibroblasts produce the rest of this protein. Hence, they are the target cells for the therapy approaches.

In order to test the ability of adenoviral vectors to transduce and the performance of Cas9 protein in term of mutated exon deletion, keratinocytes and fibroblasts carrying c.6527insC mutation were extracted from a patient to build simple 2D culture models.

Once the cells were transduced with adenoviral HD vectors that carry Cas9 gene, the viruses infect the cells and introduce the viral genome into the nucleus. In this way, the cells produce Cas9 protein that can cut the DNA at the site recognized by guidance sequence. Therefore, the first step is to confirm that they actually entered into the host cells and made then synthesize the Cas9 through fluorescent light emission observation (Figure 22).

2.1. Transduction

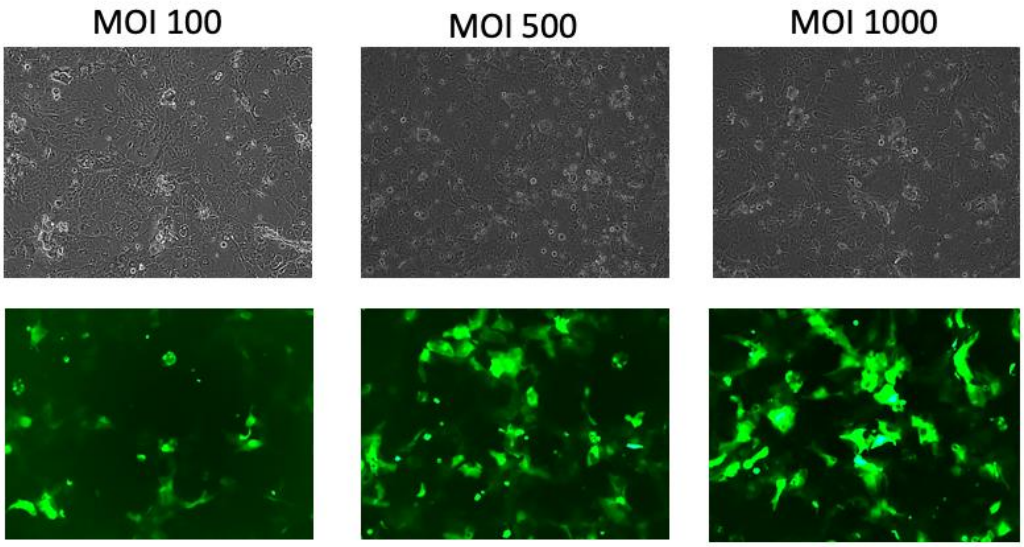

Figure 22. Bright field image and green fluorescence of transduced patient keratinocytes with HD adenoviral vectors at different MOI at day 6. Magnification: 20X.

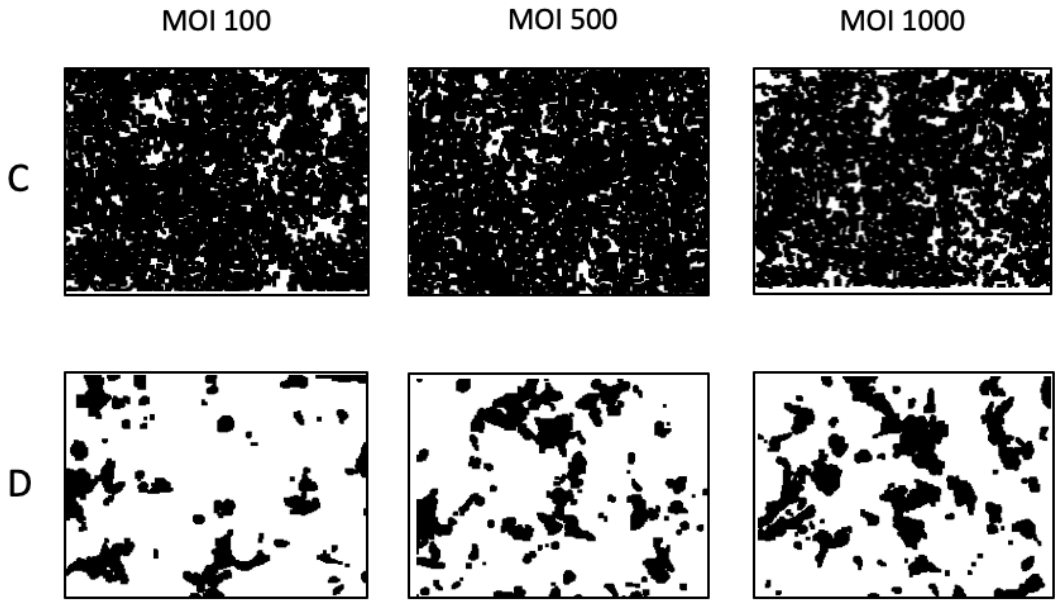

Figure 23. Segmented images are binary images. The background (white) is labeled with the lowest pixel value while the cells (black) are labeled with the height pixel value.

In the bright field images in Figure 22, the cells were identified with keratinocytes morphology but neither the infection nor the production of gene editing proteins could be observed. Fluorescence emission of these cells provided this information. The viral genome delivering the cassette of Cas9 and GFP was incorporated into the host cell nucleus. Therefore, the presence of green fluorescence protein implies the successful infection and production of the nuclease.

The brightfield images segmentation task was more difficult due to the complex texture and varied intensities in the edges. From the original images, we could say that the confluency is similar at the three different MOI, while there was a clear difference in the fluorescence area and intensity according to Figure 23. As no nucleus staining was used, cell counting was not possible, so the transduction efficiency was based on the fluorescence area with respect to the confluency.

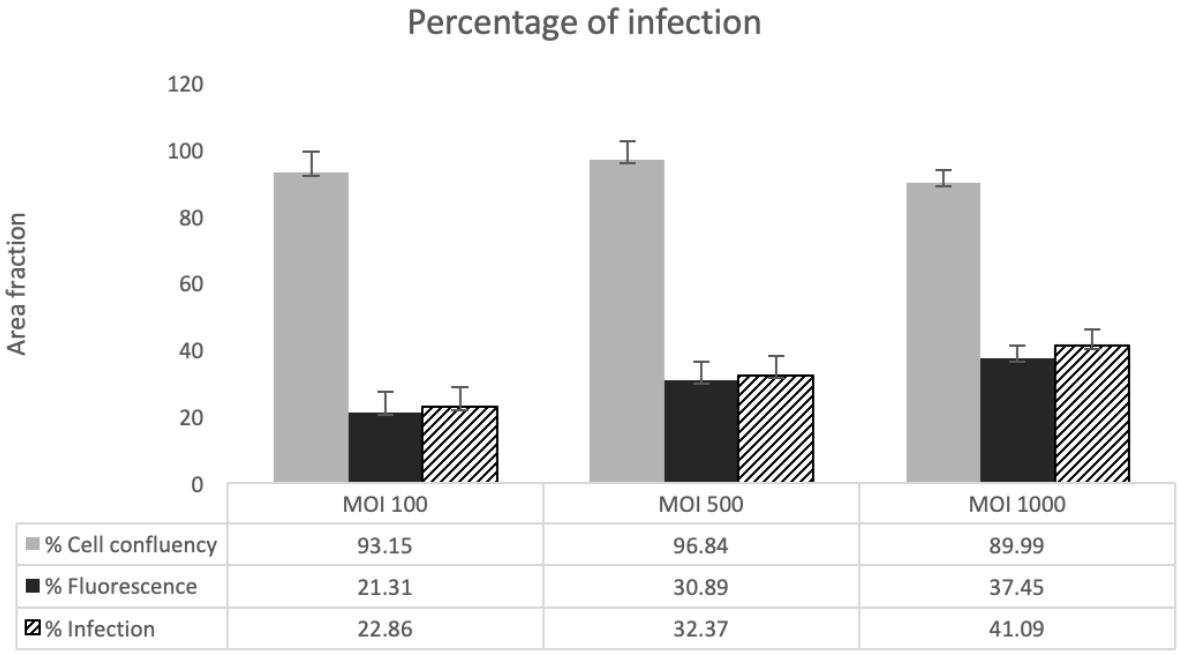

	MOI 100	MOI 500	MOI 1000
% Cell confluency	93.15	96.84	89.99
% Fluorescence	21.31	30.89	37.45
% Infection	22.86	32.37	41.09

Figure 24. Infection ratio calculated basing on the cell confluency and fluorescence area percentage with the program ImageJ.

The area of fluorescent keratinocytes increases as the MOI rises as plotted in Figure 24. From Figure 23, an increased intensity could also be observed. Focusing on bright field of the MOI 1000 showed in Figure 23, most of keratinocytes were attached to the bottom according to their morphology, which means they were alive, because dead keratinocytes were rounded and detached from the plate. However, this high infection did not cause a larger toxicity to the cells as keratinocytes confluency is similar to those infected at MOI 100 and 500. The toxicity was further discussed in another section with Figure 33 and 34.

Even the fluorescence revealed the production of Cas9, the activity of this nuclease could not be determined, that is, the presence of Cas9 could not ensure the deletion of exon 80. Therefore, DNA analysis should be carried out in order to study the Cas9 performance in term of exon 80 deletion.

2.2. PCR analysis

DNA was extracted from infected keratinocytes and fibroblasts and underwent polymerase chain reaction (PCR). The small segment, amplified by PRC, exclusively contained introns 79 and 80, and exon 80 according to the primers R and F1, with a total length of 493 bp.

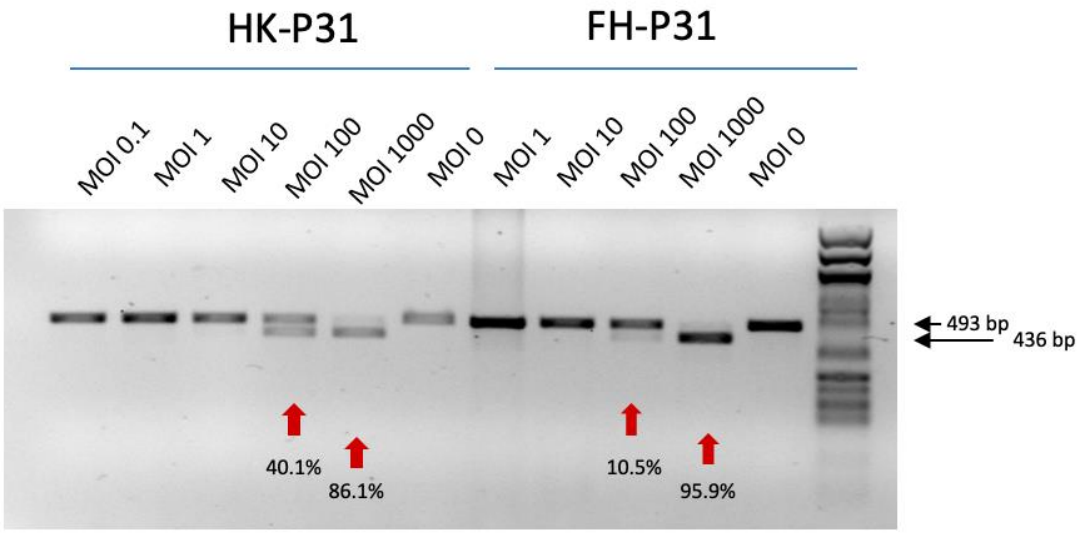

Figure 25. The evaluation of the Cas9 activity on the patient keratinocytes (HK) and fibroblasts (FH) transduced with HD with increasing MOI. In the middle, the control (MOI 0) is found and represents the intact DNA fragment, while at the end, weight marker indicates that the DNA fragments were correctly amplified.

There are two different molecular weight levels where the bands are localized. The DNA molecule suffering deletion has a shorter length (436 bp) such that it migrates faster and, therefore travelling longer distance, it is found in the lower level. The band derived from the culture without being infected serves as a negative control of the weight of uncut fragment and is retained in the higher level.

Deletion of exon 80 was observed in the keratinocytes and fibroblasts transduced with MOI 100 and 1000, as the red narrows indicate. For both types of cells, the result was better as the MOI increases, that is, more viral particles (1000 particles) transducing a single cell. This is based on the fact that the top band intensity decreases and that of the bottom band increases.

For the rest of cultures transduced with lower concentration, such as MOI 0.1, MOI 1 and MOI 10, the DNA was not edited by the Cas9.

3. 3D culture gene editing

Organotypic culture is a powerful tool to mimic the skin due to its 3D structure and were used in many studies for Cas9 activity assessment. Thanks to the fibrin hydrogel embedding fibroblasts and the air-liquid interface, the keratinocytes could migrate and differentiate in response to the provided mechanical and chemical stimuli to form multilayered epithelium. The blister was formed (Figure 26.A) through needle that injected air into the hole created on the epidermis. Then the HD adenoviral particles were injected into the blister (Figure 26.B). This model mimics the blister in the RDEB patients, so we think it is a good model to assess the treatment.

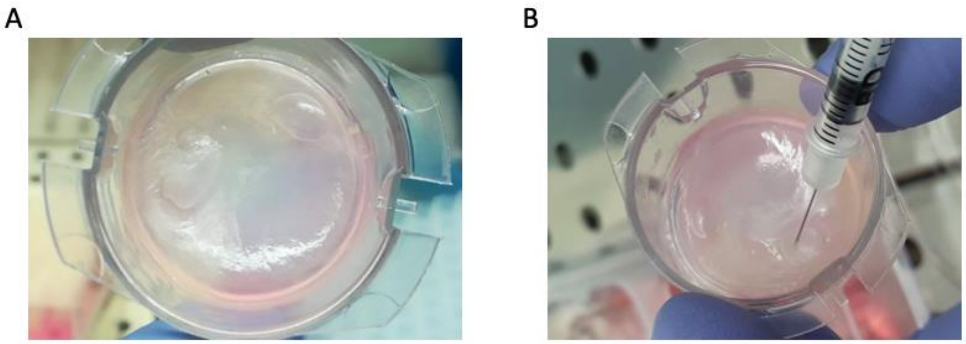

Figure 26. Blister formation and viral vectors injection. A hole is made on the epidermis layer and the air enters through needle and breaks the adhesion between epidermal and dermal layer. Then different types of viral vectors were injected in the corresponding organotypic cultures.

3.1. Transduction

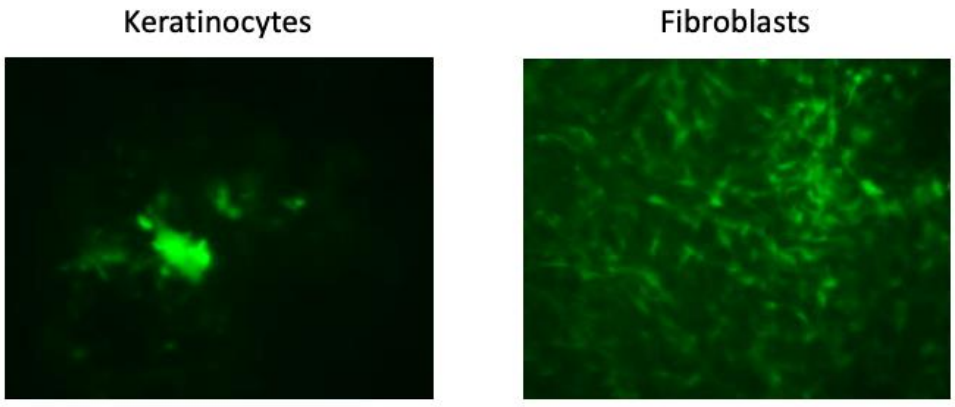

Figure 27. Fluorescence observation at day 4 of HD adenoviral vectors injection into the blister. There are two layers of organotypic culture, being the keratinocytes in the top epidermal layer and fibroblasts in the bottom dermal layer. Magnification: 20X.

Both keratinocytes in epidermis and fibroblasts in dermis were infected. The difference between fluorescence distribution in Figure 27 is due to the different vertical planes during microscopic observation.

3.2. PCR analysis

The PCR analysis obtained from amplified DNA extracted from the organotypic cultures is showed in Figure 28. It starts with the molecular weight marker, followed by the negative control (without transduction) and the positive control (corrected cells in 2D culture). The control organotypic culture was not infected and, therefore, neither epidermis nor dermis presented deletion. In the infected cultures, the epidermis genome did not suffer edition, as there was no band at the position of bottom band of positive control which contains 50% cells with exon deletion.

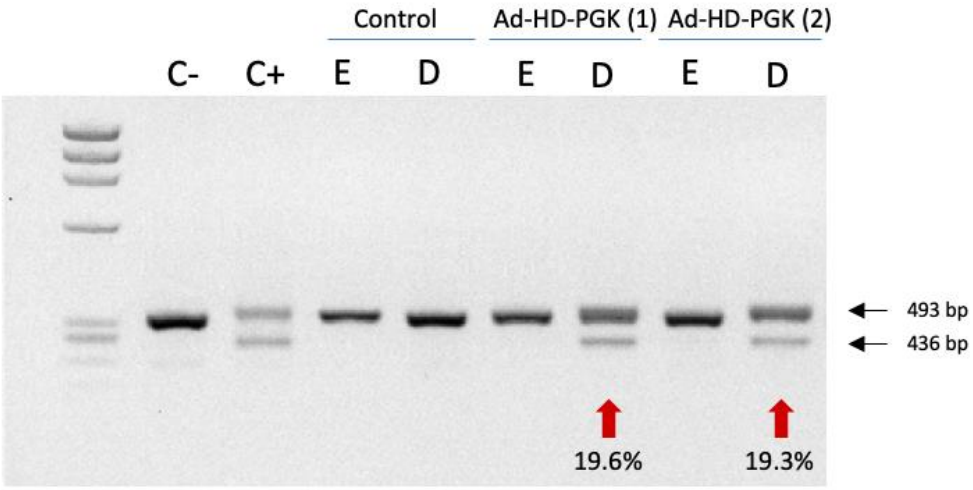

Figure 28. Evaluation of the performance of sgRNA-Cas9 on the organotypic culture having blister injected with HD adenoviral vectors. C- is negative control, C+ is control with 50% deletion, E stands for epidermis and D for dermis.

A blister formation separating the epidermal and dermal layer could cause an abrupt damage on the basal layer of keratinocytes. Without the nutrients and signals provided by the dermis, the keratinocytes could not proliferate. Even the keratinocytes were infected by the viral vectors, they could not be edited because they did not proliferate.

This also explained why fluorescence was observed in keratinocytes (epidermis) at 4 days after virus injection into blister (Figure 27) but no correction was achieved (Figure 28). In contrast, the fibroblasts were more independent from the keratinocytes for proliferation, such that once transduced, they could still divide and be edited.

4. Graft *in vivo* gene editing

The graft take rate consisted of 8 weeks, which were necessary for the regenerative skin to become mature and completely taken into the mouse skin. During this take process, keratinocytes of the organotypic differentiated and acquires the squamous stratified organization. Then the vacuum device caused the separation of the epidermis from the dermis to form a small blister (Figure 29), into which the viral vectors were injected. Several days later, the mice were observed through fluorescence microscopy in term of *in vivo* infection (Figure 30).

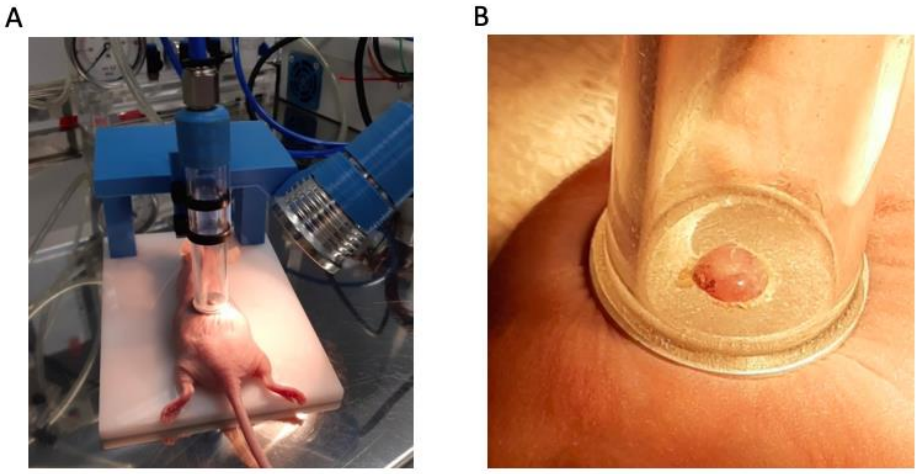

Figure 29. An anesthetized mouse placed on the device to generate a blister on the human skin graft.

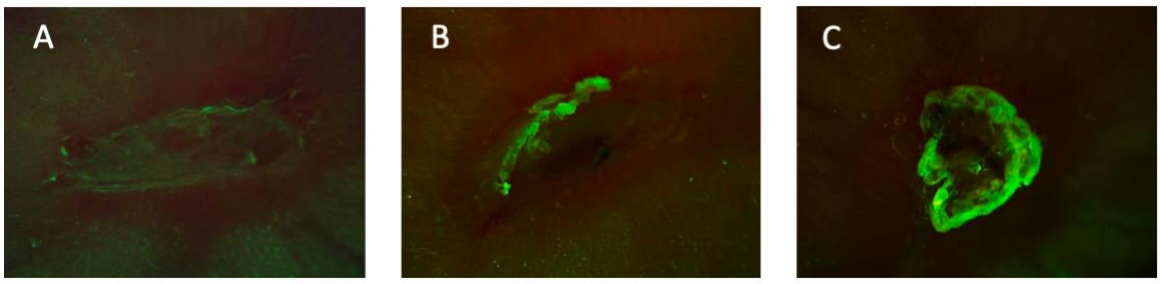

Figure 30. Fluorescence images of three implanted skin grafts. HD adenoviral vectors were injected into the blister made by the vacuum device. A) Observation at day 10 of infection. B) Observation at day 9 of infection. C) Observation at day 7 of infection.

In the first graft (Figure 32, A), there is no vivid green fluorescent light, the weak green light might be the autofluorescence of the cells. In the second graft (B), an area at the boundary of implanted skin equivalents could be clearly identified with more intensive green fluorescence. The last graft (C) had the largest area with fluorescence, especially at the whole boundary.

5. Cytotoxicity of HD and first generation adenoviral vectors

Previous researches in the laboratory with first generation adenoviral vectors showed a high toxicity *in vitro* assessment.

Our hypothesis was that HD vectors would be less toxic because they lacked almost all viral genome, the expression of which could be toxic for transduced cells. In order to confirm that, these two different generations of adenovirus were applied to infect keratinocytes cultures at different MOI under same conditions. At day 6 of infection, they were collected for FACS analysis.

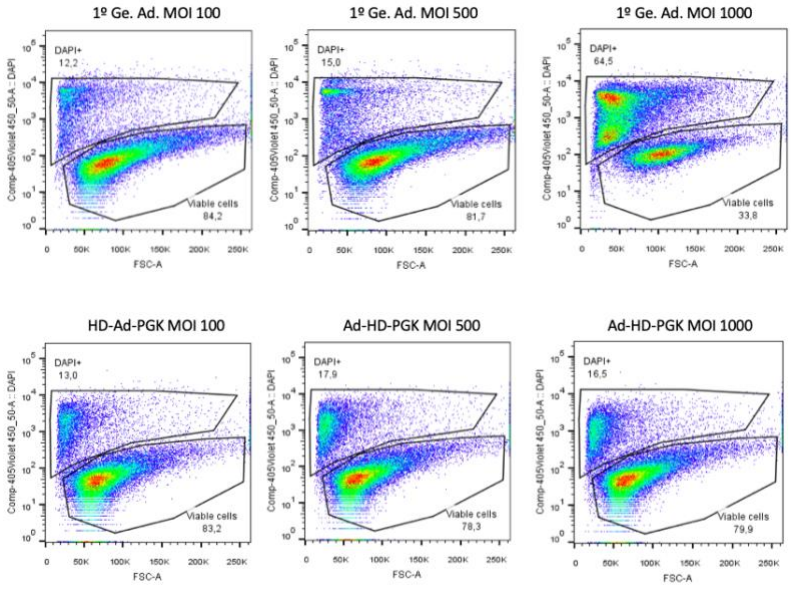

Figure 31. Toxicity assessment of two types of adenoviral vector on patient keratinocytes at day 6 of infection. Dot plots represent the fluorescence intensity of DAPI (vertical axis) against the FSC area (horizontal axis).

The FSC area of the plots in Figure 31 is the forward scatter intensity, which is proportional to the cell diameter. The intensity of DAPI is proportional to the amount of DAPI stain taken by the cells. As dead cells have more permeable cell membrane, they express blue staining with higher intensity. Therefore, those cells expressing DAPI intensity higher than the threshold are classified as dead cells (DAPI+ %). The percentage of viable cells is also labeled in the plot.

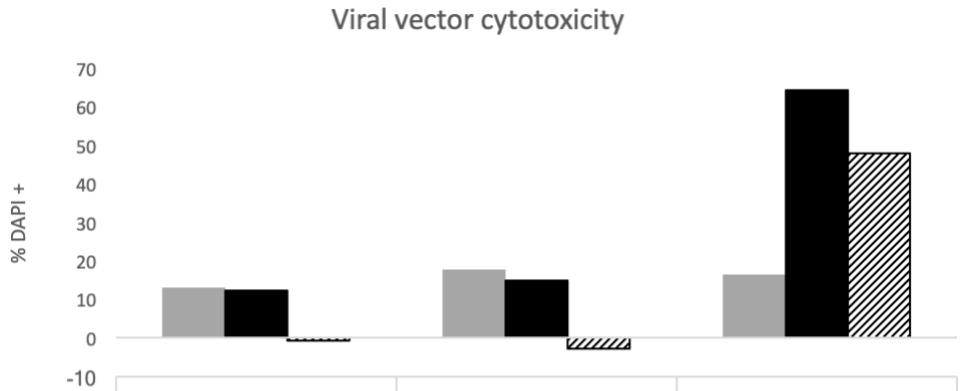

	MOI 100	MOI 500	MOI 1000
HD Ad.	13	17.9	16.5
1st Gen.	12.2	15	64.5
1st - HD	-0.8	-2.9	48

Figure 32. Numerical representation of DAPI positive cell percentage obtained from Figure 31. The plain columns belong to the HD (gray) and first generation adenoviral vectors (black), while the stripe column is the difference between first and HD vector cytotoxicity.

In both the culture infected with MOI 100 and MOI 500, the HD and the first generation vectors have similar DAPI%, being that of HD one even slightly higher than the first generation (Figure 32). Nevertheless, the fluorescence increased dramatically in the case of cells infected with first generation vectors at MOI 1000. Meanwhile, the DAPI fluorescence of those infected with HD vectors slightly decreased, showing that HD vectors are less toxic. Moreover, PCR analysis results from HD and first generation infecting keratinocytes in 2D culture are compared. With multiplicity of infection lower than 3000 of first generation vectors, no deletion on the exon 80 was observed, as showed in Figure 34, while the deletion was observed with MOI 100 of HD vectors (Figure 25).

DISCUSSION

The genome editing tool used in our study is the sgRNA-Cas9 complex, the cassette of which is delivered by helper-dependent adenoviral vectors. Even the Cas9 derived from Streptococcus pyogenes is the most commonly used type, the Staphylococcus aureus was chosen because of a more specific PAM and smaller molecular weight, which could result in less off-target activity of Cas9 protein.

After the double-strand break (DSB) caused by Cas9 protein, DNA repair through NHEJ occurred due to the lack of homologous template. As Cas9 could cause both blunt and sticky ends, being the NHEJ less accurate in blunt cuts. This is because during the repair at the endpoints, known deoxyribonucleotides could be added to the sticky cut ends, while random ones would be added to the blunt ends. But in both cases, small insertions and deletions (indels) could be introduced. It is worth noting that the two DSB occurred in the intron 79 and intron 80 in the gene *COL7A1*, because the two guide RNA were designed to target the exon 80. Thanks to the collagen specifically repeated organization, the normal function of this protein will be restored if the reading frame has been corrected. As there are only three possible reading frames (because 3 units forming a codon), at least one third of cells with E80 deletion would synthesize normal collagen VII.

But the delivery system determines the number of cells that can be modified, they way we introduce the therapeutic RNA or DNA into the cells is also crucial. Previous studied used different systems to carry sgRNA-Cas9 complex. One method consisted of delivering the sgRNA-Cas9 in form of ribonucleoprotein into the keratinocytes through electroporation. The other one is the first generation adenoviral vectors carrying the sgRNA-Cas9 cassettes within the double-strand viral genome. This two studies are compared with the HD adenoviral vectors in this chapter.

But firstly, the difference in the results obtained from 2D and 3D cultures transduced with the HD vectors, is discussed.

1. 2D versus 3D models

Due to different culture organization, the performance of viral vectors also varied. In 2D culture, the surface of cells in small suspension is more exposed to viral particles, favoring the absorption and interaction between virus fiber and receptors on cell membrane. However, there are more barriers, even with the *in vitro* organotypic culture.

Since the serotype5 adenovirus was discovered in human lung epithelial cells, it was expected to have a higher affinity to epithelial cells including keratinocytes. This is supported by the finding that in 2D culture at a lower MOI (100), the percentage of corrected keratinocytes was higher than that of corrected fibroblasts. At MOI 1000, high percentage of correction was obtained from both cell types, which is 86.1% and 95.9% for keratinocytes and fibroblasts respectively (Figure 25).

In the case of *in vitro* organotypic infected with HD vectors, only cells in the dermis layer suffered correction. Even part of epidermis was infected according to fluorescence observation (Figure27), there was no deletion in keratinocytes that were separated from the dermis due to blister formation and did not proliferate (Figure 28).

Although the keratinocytes are the main collagen VII producer cells, fibroblasts also contribute to the epidermal and dermal adhesion by synthesizing one third of collagen VII.

According to a study of fibroblast cell therapy for RDEB, the intradermal injection of wild type fibroblasts into Collagen VII knockout mouse models increased the amount of this protein in dermal-epidermal junction 4- to 5-fold (Kern JS, 2009). Although the synthesis of collagen VII lasted less than 4 weeks, the already produced protein could maintain the adhesion between epidermis and dermis, which was able to resist mechanical forces.

Not only in mice model, the RDEB patients were treated with allogeneic fibroblasts from one of their parents through intradermal injection (TracyWong, 2008). Later assessment found an increased collagen VII and anchoring fibrils synthesis from 2 weeks to 3 months after treatment.

Additionally, a research found that the Collagen VII half-life (the time after which the amount of the protein decreases by 50%) in murine skin was about one month, which is considerably long compared with other collagen types (Tobias Kuˆhl, 2016). The researchers also found that single collagen VII half-life is several times shorter than that of anchoring fibril. It seems that once these extracellular proteins are secreted and integrated into the DEJ, where they form the anchoring fibrils through cross-linking by transglutaminase. Hence, the fibril is more stable than single collagen protein, so that it is also more resistant to degradation.

The successful synthesis of Collagen VII through normal fibroblasts injection and the high stability of both protein and the resulting anchoring fibril were achieved. Based on this, we expect that during *in vivo* gene editing, the infected fibroblasts with E80 deletion and with restored *COL7A1* expression could synthesize enough amount of collagen to form the anchoring fibrils and support the keratinocytes reepithelialization in a long period of time.

2. Viral versus non-viral delivery system

The previous study (Jose Bonafont, 2019) consisted in delivery sgRNA-guided Cas9 nucleases through nucleofection into the RDEB keratinocytes as a novel delivery system, because it is the nuclease itself being delivered. There were four different sgRNA pairs associated with the ribonuleoprotein complexes in order to test which pair could yield the best result.

sgRNA pairs	Distance between cutting sites
sg2+sg4	56 pb
sg1+sg3	191 bp
sg2+sg3	55 bp
sg1+sg4	192 bp

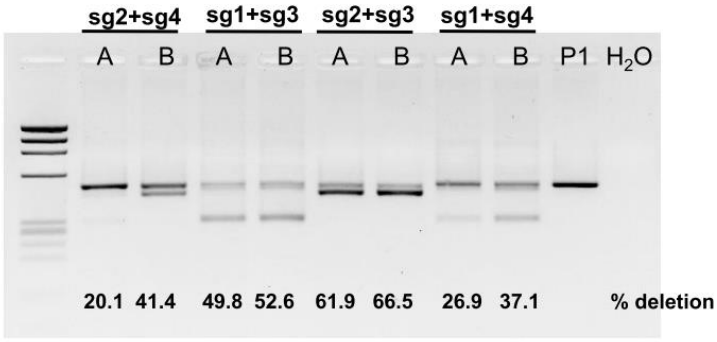

Figure 33. PCR analysis of DNA from keratinocytes treated with ribonucleoprotein complexes. The deletion ratios were obtained through densitometry. Two nucleofection conditions were tested and referred as A and B. P1 represents the unedited keratinocytes from a patient (Jose Bonafont, 2019).

From the results obtained through PCR analysis (Figure 34), keratinocytes treated with sg2+sg3-Cas9 nucleases have the highest deletion percentage (61.9% and 66.5%). It is important to recall that the deletion percentage in keratinocytes infected with HD vectors at MOI 1000 was 86.1% showed in Figure 25. In both delivery systems, the ratio of edited alleles is higher than 50%.

Furthermore, the immunofluorescence analysis with a specific anti-C7 antibody showed the expression of Collagen VII in 81% RDEB keratinocytes treated with sg2+sg3-Cas9 nucleases. The successful long-term engraftment was also achieved by using polyclonal populations of RDEB keratinocytes with E80 deletion, which suggests that epidermal stem cells were edited.

All these compromising results obtained in this *ex vivo* correction of RDEB keratinocytes encouraged the use of HD adenoviral vectors carrying sgRNA-Cas9 cassette for *in vivo* gene editing therapy.

3. *In vivo* versus *ex vivo* gene therapy

Unlike the internal organs, skin is exposed to air and can be easily accessed and treated with corrected cells transplantation. Therefore, the most commonly used method for skin is *ex vivo* therapy, with a vast number of studies proving the high delivery efficiency. However, this approach starts from taking the patient biopsy, followed by extraction of specific cells, correction, amplification, differentiation and, finally, transplantation. The whole process is time-consuming. In contrast, *in vivo* therapy is fast, because it simply consists of injection of vectors carrying the transgene, without any cell manipulation.

However, these vectors find much more physiological barriers when they are injected directly than when they are applied to cell suspension, so that the uptake efficiency is relatively lower. Another difficulty is the immune response caused by viral vectors.

The first-generation vectors were not considered as a good candidate for the *in vivo* gene therapy for the following reasons. These viruses are also replication-deficient vectors, due to the E1 regions removal to prevent E2 gene expression, and also need to be produced in complementing human cell lines (293 cells) that provided the genes necessary for replication. However, after gene editing, the viral genome still remained inside the host cells and its expression resulted in viral proteins that are toxic. In addition to the high toxicity, the deletion in keratinocytes infected with these vectors was observed from MOI equal or higher than 3000 (Figure 34). Therefore, 30 times more first generation viral particles would be needed to achieve a similar correction ratio in HD viral particles, as this type achieved deletion with MOI 100 (Figure 25).

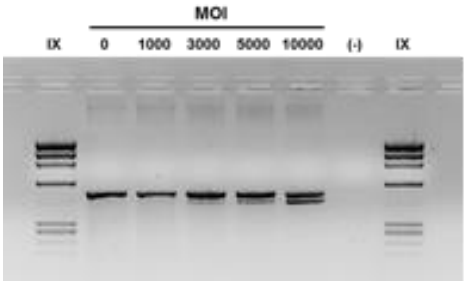

Figure 34. PCR analysis of DNA from keratinocytes infected with first generation adenoviruses with different MOI (previous result in the research center).

Furthermore, the synthesized viral proteins would be exposed on the transduced cell membrane and, in this case, would induce immune response by attracting T cells and natural killers. Subsequently, the target cells would be destroyed. In contrast, the genome of HD is mainly composed of stuffer sequence that do not result in protein. In this way, the use of HD vectors is safer and less immunogenic.

CONCLUSSION

- High concentration of Helper-Dependent adenoviral vectors was obtained after serial passage, amplification and ultracentrifugation

- In 2D culture model, exon 80 deletion in *COL7A1* gene occurred at MOI 500 and MOI 1000, being the last with that yield 86% and 96% deletion in keratinocytes and fibroblasts respectively

- In the organotypic culture consisting of fibroblasts embedded in fibrin gel and keratinocytes seeded on the top, the blister was formed to mimic the situation of RDEB patients, and then treated with HD vectors. According to the PCR analysis, exon 80 deletion was only observed in fibroblasts

- More realistic models of RDEB patients skin were created through skin equivalent maturation once transplanted in immunodeficient mice, while the blister was formed with vacuum device. The presence of green fluorescence from the graft on the mouse proved that cells in the blister were successfully infected

- The toxicity analysis demonstrated our hypothesis that HD vectors would be less toxic than the first generation vectors due to the lack of almost all viral genome. This was possible thanks to the presence of helper adenoviruses during production and amplification. In this way, after the genetic modification, no viral protein will be produced inside the host cells

- The MOI needed to cause the exon 80 deletion is reduced from MOI 3000 (first generation adenoviruses) to MOI 100 with HD, that is less number of viral particles can be used to achieve the same therapeutic effect, which could further decrease the toxicity and immune response

CHALLENGES AND FUTURE WORK

- As the promoter is PGK, which is expressed in almost all human cell types, the gene editing would be carried out in any human cell. During *in vivo* viral vectors administration, cells different to keratinocytes and fibroblasts could be infected and suffer exon 80 skipping. Even they do not actively produce collagen VII, genetic modification can somehow threaten the DNA molecules. The next step is to produce a HD adenoviral vector that only allows the Cas9 expression in a single cell type. This can be achieved by using, for instance, the promoter that regulates keratin 5, which is only expressed in keratinocytes.

- A deeper understanding on the kinetics of Cas9-sgRNA complex and the stability of the transgene in different conditions and cell types can improve the nuclease activity and DNA correction in both *in vitro* and *in vivo* approaches

- Inactivation of Cas9 gene remaining inside the cells can prevent its off-target activity. There is a newly developed method that consists of cleaving the viral own genome encoding Cas9 by the Cas9 itself. Cas9 cuts the desired site in the DNA molecules of the host cells following one of the sgRNA, and also cuts the Cas9 gene of viral genome under the direction of the other sgRNA (Donna J.Palmer, 2019)

- The homologous recombination can be considered for DSB repair with the introduction of a template into the viral vector design. In this method, higher percentage of corrected cells could express the *COL7A1* with the correct reading frame but without indels that could affect intron-splicing-signals.

- Another limitation is that the immune response. As serotype 5 adenoviruses are commonly causes of respiratory infections, many people have developed antibodies against the proteins forming adenoviral capsid. This is a problem *in vivo* gene therapy, where the viral vectors are directly injected into the patient body. Recently studies show that the serotype 5 capsid can be replaced by the capsid of chimpanzee serotype 35 adenovirus to avoid immune response and acute cytotoxicity (Donna J.Palmer, 2019).

REGULATORY FRAMEWORK AND SOCIECONMIC IMPACT

1. EU regulations

The final products resulting from gene therapy, along with those from tissue engineering and cell therapy, are considered as part of the Advanced Therapy Medicinal Products (ATMPs). Due to the biological components, these products are highly variable, patient-dependent and concerned about the following aspects: safety implications, ethical aspects, lack of data about therapeutic effects and low stability.

Hence, they need to be controlled by ATMP Regulation (Regulation (EC) 1394/2007). This regulation, agreed by several EU institutions, specifies many requirements, such as cell sources, pre-clinical development, risk analysis, manufacturing process and risk-based approach, allowing the traceability of each production step. The ATMPs must be carried out in an authorized center following good manufacturing practices (GMP). This continuous control aims at avoiding any error during production to ensure the safety and efficiency of the final medicinal product. Another element of this regulation consisting of registry and commercialization, allows free movement of these medicinal products within Europe and facilitates the European companies to access into this new field.

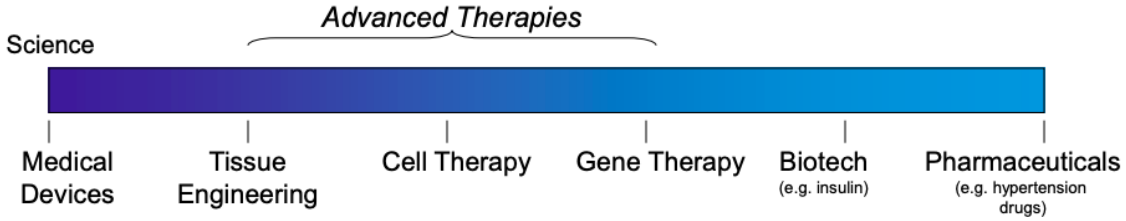

Figure 35. Advanced Therapies Medicinal Products (Celis, 2018).

The genetically modified organisms (GMO) like recombinant viral vectors and the corrected cells yielding more complex tissues must obey the Directive 2001/18/EC or Directive 2009/41/EC during clinical trials.

As the *in vivo* approach of correcting the *COL7A1* gene with adenoviral vectors is still in the experimental stage and need further research and improvement, the regulation chapters of GMP were not applied to this project. Nevertheless, it is important to have them in mind and to follow the good practice in cell culture and molecular laboratories in term of the materials, the experiment procedure and the waste management. In this way, the reproducibility and reliability of the experiment could be ensured.

In addition to the product quality that ensures the patient safety, the safety of the researchers constantly exposed to biological agents is also an important issue. In the case of inappropriate manipulation, these agents can be source of contamination and cause unexpected harm. Since genetically modified microorganisms are also considered as biological agents, their contained use regulation is linked to those applied to the Directive 2000/54/EC, the legislation on biosafety. The virus production and keratinocytes, fibroblasts and organotypic cultures were carried out in Keratolab in CIEMAT, which is a laboratory specialized in primary culture of skin cells. Equipment like the laminar flow hood of biosecurity level II forms a barrier between the cell cultures and the personal.

The skin equivalent transplantation and later fluorescence observation of *in vivo* HD adenoviral vectors performance was carried out in the CIEMAT Laboratory Animals Facility, which provides services like breeding of immunodeficient, transgenic or irradiated mice models. The animals are kept in a pathogen-free conditions while their manipulations were done obeying the regulations defined in European Convention 123, use and protection of vertebrate animals in experimentation and other scientific purposes.

2. Social responsibility

A rare disease is considered to be carried out by no more than 5 in every 10.000 people. According to estimations, there is a range of 5000 to 8000 genetic rare diseases, which is supposed to affect 6% of European population. CIBERER points out that there are around 3 million Spanish people suffering a rare disease, which affects not only children, but can also arise during an adult's life. Compared with this large number of patients, there is however few efficient commercial treatments for these diseases. Due to their high specificity and variability, large pharmaceutic companies are not interested in offering treatment for rare diseases. This responsibility has always been assumed by public research centers, among which CIEMAT plays a great role together with BIBERER in Spain in order to achieve advances in diagnostic and therapeutic approaches.

3. Project cost

Experimental Materials				
Company	Material	Cost/unit (€)	Units	Total (€)
Integrated DNA Technologies	crRNA1 2nmol	72.00	0.2	14.40
	crRNA2 2nmol	72.00	0.2	14.40
	tracrRNA 5nmol	72.00	0.5	36.00
	Cas9 nuclease 100µg	195.00	0.03	5.85
GlutaMAX™, Gibco®	DMEM 500mL	27.00	20	540.00
	F12 500mL	32.00	4	128.00
HyClone™	FBS 50mL	81.00	1	81.00
	Bovine Calf Serum 500mL	64.00	2	128.00
Sigma-Aldrich	TRYPSIN 100mL	15.00	1	15.00
	PBS 500	17.00	2	34.00
	Matrigel 1mL	139.00	0.5	69.50
	Thrombin 10 mg	139.00	0.2	27.80
	cholera toxin 10mL	301.00	0.2	60.20
	Ascorbic acid 10mL	122.00	0.2	24.40
	insulin 10mL	111.00	0.2	22.20
	antibiotics 100µL	340.00	0.1	34.00
Thermo Scientific™	TAE 50x 1L	34.00	0.1	3.40
Amchafibrin, FidesEcofarm	tranexamic acid 10mL	315.00	0.2	63.00
			Total	1357.35

Experimental Disposables

Company	Material	Cost/unit (€)	Units	Total (€)
Fischer Scientific	Petri dish 150mm 500u	390.00	0.2	78.00
	Petri dish 60mm 500u	390.00	0.2	78.00
	Petri dish 35mm 500u	428	0.1	42.80
	Plate 6 wells 50u	132	0.1	13.20
	Transwell 60u	305.00	0.5	152.50
	Stripette 1.5mL 500u	45.00	0.2	9.00
	Stripette 2mL 200u	67.00	1	67.00
	Stripette 5mL 200u	67.00	1	67.00
	Stripette 10mL 200u	67.00	0.5	33.50
	Stripette 25mL 200u	67.00	0.5	33.50
			Total	574.50
			Total cost of project	1931.85

BIBLIOGRAPHY

Čepa, M. (19 de November de 2018). Segmentation of Total Cell Area in Brightfield Microscopy Images. *MDPI*, 0.

Alex Reis, P. B. (2014). CRISPR/Cas9 & Targeted Genome Editing: New Era in Molecular Biology. *NEB expressions Issue I*, 0.

Atum M Buo, M. S. (09 de August de 2016). A cost-effective method to enhance adenoviral transduction of primary murine osteoblasts and bone marrow stromal cells. *Nature*(16021), 0.

B.R. Grubb, R. P. (1994). Inefficient gene transfer by adenovirus vector to cystic fibrosis airway epithelia of mice and humans. *Nature, 371*(6500), 802-806.

Bremer J, B. O. (2016). Antisense oligonucleotide-mediated exon skipping as a systemic therapeutic approach for recessive dystrophic epidermolysis bullosa . *Molecular Therapy - Nucleic Acids*.

Celis, P. (2018). ATMPs and ATMP Regulation. *RD-ACTION, European Medicines Agency, and European Commission-DG SANTE workshop: how European Reference Networks can add value to clinical research* (pág. 7). EU: 2018.

Chen L, A. M. (1996). Production and characterization of human 293 cell line expressing the site-specific recombinase Cre. *Somatic Cell and Molecular Genetics*, 477-88.

Christelle Bonod-Bidaud, F. R. (2013). Inherited Connective Tissue Disorders of Collagens: Lessons from Targeted Mutagenesis. *intechopen*, 0.

Corneli Doebis, T. R.-D. (2 de May de 2002). Efficient in vitro transduction of epithelial cells and keratinocytes with improved adenoviral gene transfer for the application in skin tissue engineering. *Transplant Immunology*, 323-329.

Cory L. Simpson, D. M. (2011). Deconstructing the skin: cytoarchitectural determinants of epidermal morphogenesis. *Molecular cell biology, 12(9)*, 565-80.

Cristina Chamorro, A. M. (2016). Gene Editing for the Efficient Correction of a Recurrent COL7A1 Mutation in Recessive Dystrophic Epidermolysis Bullosa Keratinocytes. *Official journal of the American Society of Gene & Cell Therapy*, 307.

Cutlar L, G. Y. (04 de January de 2016). A knot polymer mediated non-viral gene transfection for skin cells. *Biomater Science*, 92-95.

De-Gui Wang, M.-J. Z.-Q.-W.-T.-F.-X. (1 de November de 2016). Fiber-modified adenovirus-mediated suicide gene therapy can efficiently eliminate bladder cancer cells in vitro and in vivo . *Oncotarget, 7*(44), 71710-71717.

Donna J.Palmer, D. L. (14 de June de 2019). Production of CRISPR/Cas9-Mediated Self-Cleaving Helper-Dependent Adenoviruses. *Methods & Clinical Development, 13*, 432-439.

Elisa Cimetta, M. F. (4 de June de 2012). Microfluidic-driven viral infection on cell cultures: Theoretical and experimental study. *Biomicrofluidics*, 024127.

Ellen G Pfendner, P. a. (21 de August de 2006). Dystrophic Epidermolysis Bullosa. *GeneReviews®*, 0.

Emmanuelle Charpentier, J. A. (06 de March de 2013). Rewriting a genome. *Natural, 495*, 50-51.

EU Clinical Trials Register. (18 de September de 2017). *Clinical trials*. Obtenido de EudraCT Number: 2017-000606-37: https://www.clinicaltrialsregister.eu/ctr-search/trial/2017-000606-37/ES#B

Georgiadis C, S. F. (2016). Lentiviral engineered fibroblasts expressing codon-optimized COL7A1 restore anchoring fibrils in RDEB. *Journal of Investigative Dermatology*, 136:284–292.

Jane Flint, V. R. (2015). *Principles of Virology, Fourth Edition.* Washington: American Society For Microbiology.

Jane Flint, V. R. (2015). *Principles of Virology, ASM Press.* Washington: ASM Press.

Jinek M, C. K. (17 de Aug de 2012). A programmable dual-RNA-guided DNA endonuclease in adaptive bacterial immunity. *Science, 337*(6096), 816-621.

Jose Bonafont, A. M.-S.-H. (May de 2019). Clinically Relevant Correction of Recessive Dystrophic Epidermolysis Bullosa by Dual sgRNA CRISPR/Cas9-Mediated Gene Editing. *Molecular Therapy, 27*(5), 986-998.

Kern JS, L. S.-T. (19 de September de 2009). Mechanisms of fibroblast cell therapy for dystrophic epidermolysis bullosa: high stability of collagen VII favors long-term skin integrity. *Molecular Therapy*, 1605-1615.

Kim YG, C. J. (6 de Feb de 1996). Hybrid restriction enzymes: zinc finger fusions to Fok I cleavage domain. . *PNAS, 93*(3), 1156-1160.

Lee, J. S. (2013). Comparison of Gene Expression Profiles between Keratinocytes, Melanocytes and Fibroblasts. *Annals of dermatology*(25), 36-45.

Lehrman, S. (1999). Virus treatment questioned after gene therapy death. *Nature, 401*, 517-518.

Lucas F. Ribeiro, L. F. (2 de August de 2018). Protein Engineering Strategies to Expand CRISPR-Cas9 Applications. *International Journal of Genomics*, 0.

lukemiller.org. (4 de November de 2010). *Miscellaneous topics vaguely related to science.* Obtenido de Analyzing gels and western blots with ImageJ: https://lukemiller.org/index.php/2010/11/analyzing-gels-and-western-blots-with-image-j/

Lundstrom, K. (2018). Viral Vector in Gene Therapy. *MDPI Disease*, 42.

MARCELA DEL RIO, F. L. (2002). A Preclinical Model for the Analysis of Genetically Modified Human Skin In Vivo. *HUMAN GENE THERAPY*, 959-968.

Michael Vanden Oever, K. T. (01 de November de 2017). Inside out: regenerative medicine for recessive dystrophic epidermolysis bullosa. *Pediatric research*, 318–324 .

Murali Ramamoorth, A. N. (2015). Non Viral Vectors in Gene Therapy- An Overview. *Journal of Clinical and Diagnostic Research*, 9,1.

National Library of Medicine (US). (16 de September de 2013). *Genetics Home Reference*. Obtenido de Gene therapy using an adenovirus vector: https://ghr.nlm.nih.gov/primer/illustrations/therapyvector

Peter C. van den Akker, M. F.-T. (2011). The international dystrophic epidermolysis bullosa patient registry: An online database of dystrophic epidermolysis bullosa patients and their COL7A1 mutations†. 0.

Philip Ng, F. L. (1999). *Gene Therapy Protocols 2nd Edition.* Totowa, NJ: Humana Press Inc.

Poyo, C. C. (2016). *Development of biosecurity protocols in gene editing for the correction of recessive dystrophic epidermolysis bullosa.* Madrid, Madrid, Spain: CIEMAT, CIBERER, UC3M.

Robin J. Parks, L. C. (26 de November de 1996). A helper-dependent adenovirus vector system: Removal of helper virus by Cre-mediated excision of the viral packaging signal. 13565-13570.

S, V. C. (2004). Adenoviral vectors for gene transfer and therapy. *The journal of gene medicine*, 164-171.

Shimizu, H. (2007). *Shimizu's Textbook of Dermatology.* Sapporo, Japan: Hokkaido University Press.

Suresh K. Mittal, A. S. (2011). Adenoviral Vectors: Potential and Challenges as a Gene Delivery System. *Department of Comparative Pathobiology, Purdue University Center for Cancer Research, and Bindley Bioscience Center*, 10-20.

Technology for Genetic Analysis. (14 de Feruary de 2012). *DNA Sequencing and Fragment Analysis*. Obtenido de DNA fragments resolve better on correct percent agarose gel.

Tobias Hirsch, T. R. (16 de November de 2017). Regeneration of the entire human epidermis by transgenic stem cells. *Nature, 551*(7680), 327-332.

Tobias Ku¨hl, M. M.-T. (June de 2016). Collagen VII Half-Life at the Dermal-Epidermal Junction Zone: Implications for Mechanisms and Therapy of Genodermatoses. *Investigative Dermatology, 136*(6), 1116-1123.

TracyWong, L. L.-H. (September de 2008). Potential of Fibroblast Cell Therapy for Recessive Dystrophic Epidermolysis Bullosa. *Investigative Dermatology, 128*(9), 2179-2189.

W.Pelley, J. (2012). *Elsevier's Integrated Review Biochemistry* . Texas: Mosby. Obtenido de ScienceDirect: https://www.sciencedirect.com/topics/biochemistry-genetics-and-molecular-biology/frameshift-mutation